Continuum Mech. Thermodyn. (2014) 26:593–618
DOI 10.1007/s00161-013-0320-y

ORIGINAL ARTICLE

Michael J. Fryer · Henning Struchtrup

Moment model and boundary conditions for energy transport in the phonon gas

Received: 7 June 2013 / Accepted: 21 August 2013 / Published online: 3 September 2013

Abstract Heat transfer in solids is modeled in the framework of kinetic theory of the phonon gas. The microscopic description of the phonon gas relies on the phonon Boltzmann equation and the Callaway model for phonon–phonon interaction. A simple model for phonon interaction with crystal boundaries, similar to the Maxwell boundary conditions in classical kinetic theory, is proposed. Macroscopic transport equation for an arbitrary set of moments is developed and closed by means of Grad's moment method. Boundary conditions for the macroscopic equations are derived from the microscopic model and the Grad closure. As example, sets with 4, 9, 16, and 25 moments are considered and solved analytically for one-dimensional heat transfer and Poiseuille flow of phonons. The results show the influence of Knudsen number on phonon drag at solid boundaries. The appearance of Knudsen layers reduces the net heat conductivity of solids in rarefied phonon regimes.

Keywords Phonon heat transfer · Moment method · Slip boundary conditions

1 Introduction

There has been an increasing focus in the last two decades on miniaturization, as scientists and engineers aim to utilize the benefits of micro- and nanotechnology. In order to effectively design devices at the corresponding length scales, it is important to understand the governing equations. As length scale decreases, different effects become more dominant and others might become less, such that approximations used in classical macroscopic theories loose validity. As a result, well-known relations, such as Fourier's law for heat conduction and the Navier–Stokes equations, begin to break down in certain regimes.

Understanding temperature and heat transfer is important for determining virtually any other property in a material, such as viscosity, electrical and thermal conductivity, heat capacity, elasticity, and ductility. Furthermore, the small size of an object and its resultant tiny thermal mass combined with the relative power of lasers can lead to huge fluctuations in temperature over short periods of time. Understanding temperature and heat transport will improve the sensitivity of sensors and could also be used for more effective thermal management of miniaturized devices, including semiconductor systems [1].

Heat in a solid is caused by vibrations of particles in the crystal lattice with respect to their mean position. These vibrations can be quantized into quasiparticles known as phonons [2,3]. Macroscopic properties such as temperature, internal energy, and heat flux can be determined by analysis of the phonon properties, such as energy and quasimomentum. Heat and temperature properties of systems can be determined by tracking all phonons in a domain (i.e., by molecular dynamics), but this can be prohibitively expensive when large numbers

Communicated by Andreas Öchsner.

M. J. Fryer · H. Struchtrup (✉)
Mechanical Engineering, University of Victoria, Victoria, BC, Canada
E-mail: struchtr@uvic.ca

of phonons are present. The direct simulation Monte Carlo method (DSMC), which uses a statistical approach to groups of particles, can be used in situations where large numbers of phonons are present, but it can still be computationally expensive [4].

Another approach is to extend the classical heat transport equations—i.e., Fourier's law—by using phonon kinetic theory to add terms and equations to the existing macroscopic equations. In the case of heat transport in solids, extended equations are necessary at larger (>0.01) Knudsen numbers, Kn, defined as the ratio of the mean free path of phonons, λ, to the length scale, L, of the system. The equations are extended by analyzing microscopic phonon kinetic theory and then integrating the properties to develop macroscopic equations. This approach was first used by Grad in kinetic theory of classical gases [5] and later extended to phonon kinetic theory [6].

Earlier moment models did not include a proper theory of boundary conditions, which limited the consideration of the extended transport models to few special cases [6]. Clearly, to render the macroscopic approach to phonon transport into a useful tool for simulation and understanding of devices, one needs reliable boundary conditions. Phenomenological boundary conditions to extended thermodynamic equations for phonons have recently been presented [7–9] for the Guyer–Krumhansl equations [10,11] that correspond to a 9-moment method.

In the present paper, in order to bridge between the microscopic and macroscopic descriptions of phonon transport, we present boundary conditions based on a microscopic analysis of model phonon–surface interactions. Three types of interactions are considered: isotropic scattering, specular reflection, and surface thermalization. The purpose of the model is to be versatile enough, so that proportions of the three types of interactions can be changed relative to each other to approximate experimental data.

The moment description of phonons in [6] was based on a simplified kinetic description of phonons, which we shall adhere to as well. The main simplifications are (a) a linear dispersion relation between phonon energy and momentum, (b) extension of the Brillouin zone to infinity, and (c) modeling of phonon interactions with the Callaway model [12], with frequency-independent collision frequencies. These simplifications allow relatively fast access to moment systems of arbitrary moment number. The resulting models describe the rarefied phonon gas in principle and offer parameters such as the relaxation times that can be used for fitting to experiments. We note, however, that these underlying assumptions are not valid for the description of systems at room temperature, where phonon dispersion is nonlinear, and the Brillouin zone cannot be extended to infinity. Hence, the present models are of limited use for application for many actual systems.

Since it is based on the same assumptions, the model of boundary conditions that we present here complements [6] in that it provides complete boundary conditions for the moment equations presented there. For self-consistency, we shall recall the model and development of the moment equations in some detail and then develop the appropriate moment boundary conditions for the moment systems. As a result, we present a framework of moment equations and boundary conditions for an arbitrary number of moments.

Detailed equations and boundary conditions are then presented and discussed for sets of 4, 9, 16, and 25 moments. The relation of the 4-moment model to Fourier's law, and of the 9-moment model to the Guyer–Krumhansl equations is pointed out. One advantage of the moment description of rarefied gases is that one can find analytical solutions for processes in simple geometry, which is not possible for the kinetic description through the Boltzmann equation. To show the capabilities of the equations, two simple problems are solved analytically, one-dimensional heat transfer through a finite crystal, including a case with an interface within the crystal, and heat flow in a narrow conductor with adiabatic sides, where phonon flow is similar to classical Poiseuille flow. We study generic cases by considering solutions of the dimensionless equations for a variety of dimensionless parameters. The solutions agree with Fourier's law for small Knudsen numbers, but boundary effects such as temperature jump and Knudsen layers markedly reduce overall conductivity for larger Knudsen numbers.

Our results show that the macroscopic approach to phonon transport allows the solution of boundary value problems for technically relevant processes with meaningful results. We refrain from comparison with actual experimental data, since the present kinetic model relies on too many simplifying assumptions (linear dispersion, finite Brillouin zone, constant collision frequency). While the present work proves that meaningful boundary conditions for moment systems for phonons can be derived, we believe that for accurate description of actual experiments, the model should be based on a more realistic kinetic model.

The remainder of the paper is organized as follows: In Sect. 2 we recall the basic elements of the microscopic description of phonons through the phonon Boltzmann equation with Callaway model, derive the moment equations, and use the Grad method for closure. Section 3 details the microscopic model for phonon–boundary interactions. The Grad distribution function is used to determine the appropriate boundary conditions for the

moment equations. In Sect. 4, we consider the developed general set of equations for the special cases of 4, 9, 16, and 25 moments, and Sect. 5 shows their applications to heat transfer problems. The paper closes with some final comments.

2 Kinetic theory of phonons

2.1 The phonon model

Internal energy of a crystalline solid is due to oscillations of particles from their mean position in a crystal lattice. These oscillations can be represented by quasiparticles known as phonons [13–15], so that the crystal is essentially described as a box filled with a phonon gas. Phonons with frequency ω have the energy $\hbar\omega$ and the momentum $\hbar\mathbf{k}$, where $\mathbf{k}$ is the phonon wave vector, and $\hbar$ is Planck's constant. For a phonon with given wave vector, the frequency follows from the dispersion relation $\omega(\mathbf{k})$; phonons travel with the group velocity $\mathbf{v}_g = \frac{\partial\omega}{\partial\mathbf{k}}$.

Phonon number is not conserved, since phonons can be created and annihilated in interactions. In particular, two phonons may combine to form one phonon, or one phonon may split into two phonons [13]. In both cases, energy is conserved,

$$\hbar\omega' + \hbar\omega'' = \hbar\omega''' \quad \text{or} \quad \hbar\omega' = \hbar\omega'' + \hbar\omega'''. \tag{1}$$

Phonon momentum, sometimes called quasimomentum or crystal momentum, is not always conserved, but obeys the rules

$$\hbar\mathbf{k}' + \hbar\mathbf{k}'' = \hbar\mathbf{k}''' + \hbar\mathbf{G} \quad \text{or} \quad \hbar\mathbf{k}' = \hbar\mathbf{k}'' + \hbar\mathbf{k}''' + \hbar\mathbf{G}, \tag{2}$$

where $\mathbf{G}$ is the reciprocal lattice vector. If $\mathbf{G}$ is zero, the process is known as a *normal* process, because momentum is conserved. If $\mathbf{G}$ is nonzero, the process is known as an *Umklapp* processes. Umklapp processes occur because of the periodic nature of phonon dispersion. One full period of the dispersion relation is known as the Brillouin zone. Since the relation is periodic, all phonons can be described with a frequency, ω, and a wave vector, $\mathbf{k}$, within the Brillouin zone. Any phonon with a wave vector outside of the Brillouin zone can be described as a phonon inside the Brillouin zone plus an integer multiple of $\mathbf{G}$. In this way, phonon momentum is created and destroyed [2,3].

Phonons may also interact with electrons and photons, and they are scattered at dislocations and other impurities. Also, acoustical phonons are produced from decay of optical phonons [16]. Also for these processes, quasimomentum is not conserved. For the purposes of this paper, these processes and Umklapp processes are grouped together and denoted as *resistive* processes. For a more in-depth look at the kinetic properties of phonons, see [2,3,6].

2.2 Phonon kinetic theory

Since heat transport can be described as energy transport in a phonon gas, it can also be modeled using gas kinetic theory, albeit with different rules and constraints. Phonons are fully characterized by their location in space, $\mathbf{x}$, and their wave vector, $\mathbf{k}$. The phonon distribution function $f(\mathbf{x}, t, \mathbf{k})$ is defined such that the number of phonons in an element of phase space, $\mathrm{d}\mathbf{k}\mathrm{d}\mathbf{x}$, at time t is

$$dN = f(\mathbf{x}, \mathbf{k}, t)\mathrm{d}\mathbf{k}\mathrm{d}\mathbf{x}. \tag{3}$$

The distribution function follows as the solution of the phonon Boltzmann equation, which, for a rigid body, reads [6,13]

$$\frac{\partial f}{\partial t} + \frac{\partial\omega}{\partial k_i}\frac{\partial f}{\partial x_i} = S_{\mathrm{N}}(f) + S_{\mathrm{R}}(f), \tag{4}$$

where S_{N} is the collision term for normal processes, and S_{R} is the collision term for resistive processes.

Macroscopic thermodynamic properties of the phonon system can be determined as suitable averages of the distribution function. The energy of a phonon is $\hbar\omega$, so the energy density of the phonon gas, e, is

$$e(t, \mathbf{x}) = \int_{BZ} \hbar\omega f(\mathbf{x}, \mathbf{k}, t)\mathrm{d}\mathbf{k}, \tag{5}$$

where BZ denotes the Brillouin zone of the crystal lattice structure. Similarly, the momentum of a phonon is $\hbar k_i$, so the phonon momentum density, p_i, is

$$p_i\,(t,\mathbf{x}) = \int\limits_{BZ} \hbar k_i\, f(\mathbf{x},\mathbf{k},t)\mathrm{d}\mathbf{k}. \tag{6}$$

Moreover, since the phonons move with the group velocity $\frac{\partial\omega}{\partial k_i}$, the energy flux q_i is

$$q_i\,(t,\mathbf{x}) = \int\limits_{BZ} \frac{\partial\omega}{\partial k_i}\hbar\omega f(\mathbf{x},\mathbf{k},t)\mathrm{d}\mathbf{k} \tag{7}$$

and the momentum flux—or pressure tensor—Π_{ij}, is

$$\Pi_{ij}\,(t,\mathbf{x}) = \int\limits_{BZ} \frac{\partial\omega}{\partial k_i}\hbar k_j\, f(\mathbf{x},\mathbf{k},t)\mathrm{d}\mathbf{k}. \tag{8}$$

Higher-order macroscopic properties can be determined by taking higher-order moments of f in k_i. Although these quantities do not appear in classical heat transfer, they are important for extending the transport equations beyond the realm of applicability of the classical laws of heat transfer. We present them as trace-free moments, so that they remain independent of each other [17,18]. We shall consider the general moments

$$u_{\langle i_1\cdots i_n\rangle} = \int\limits_{BZ} \hbar\frac{k_{\langle i_1}\cdots k_{i_n\rangle}}{k^{n-1}} f\,(\mathbf{x},\mathbf{k},t)\,\mathrm{d}\mathbf{k}, \tag{9}$$

where indices in angular brackets, as in $k_{\langle i_1}\cdots k_{i_n\rangle}$, denote the trace-free and symmetric part of a tensor. Obviously, we have $u_i = p_i$; with the assumption of linear dispersion in the next section, also the moments e, q_i, and Π_{ij} will be directly related to (9).

Since phonons are bosons, their entropy density is

$$\eta = -k_B \int\limits_{BZ} \left(f\ln\frac{f}{y} - y\left(1+\frac{f}{y}\right)\ln\left(1+\frac{f}{y}\right)\right)\mathrm{d}\mathbf{k}, \tag{10}$$

where y is the density of states and k_B is Boltzmann's constant. The phonon distribution function in equilibrium can be determined by maximizing entropy which yields the Bose distribution [2,6,19],

$$f_{\mathrm{Bose}} = \frac{y}{\exp\left[\frac{\hbar\omega}{k_B T}\right]-1}. \tag{11}$$

2.3 Linear dispersion and infinite Brillouin zones

Several simplifying assumptions [13–15] are used in order to present the extended transport equations. An important assumption is that the system is isotropic and homogeneous. This assumption ignores the directionality inherent to crystal lattices and models the Brillouin zone as being spherical [2]. The second assumption is that the Brillouin zone can be considered as infinitely large. This implies for the definition of the moments

$$u_{\langle i_1\cdots i_n\rangle} = \int\limits_{BZ} \hbar\frac{k_{\langle i_1}\cdots k_{i_n\rangle}}{k^{n-1}} f\,\mathrm{d}\mathbf{k} = \int\limits_{-\infty}^{\infty} \hbar\frac{k_{\langle i_1}\cdots k_{i_n\rangle}}{k^{n-1}} f\,\mathrm{d}\mathbf{k} \tag{12}$$

Another assumption, which is valid at rather low temperatures, is to approximate the dispersion relation between frequency and wave vector as a linear function,

$$\omega\,(\mathbf{k}) = ck, \tag{13}$$

where c is the Debye velocity of the solid. Then, the group velocity is

$$\frac{\partial \omega}{\partial k_i} = \frac{\partial (ck)}{\partial k_i} = c\frac{k_i}{k}. \tag{14}$$

We note that linear dispersion leads to

$$e = cu, \quad q_i = \int_{BZ} \hbar c^2 k_i f \mathrm{d}\mathbf{k} = c^2 u_i, \quad \Pi_{ij} = c \int_{BZ} \hbar \frac{k_i k_j}{k} f \mathrm{d}\mathbf{k} = c u_{\langle ij \rangle} + \frac{1}{3} e \delta_{ij}. \tag{15}$$

Hence, energy, energy flux, and phonon pressure tensor are directly related to the moments $u_{\langle i_1 \cdots i_n \rangle}$ (9). In particular, the energy flux is proportional to momentum, $q_i = c^2 p_i$.

2.4 Moments of the Bose distribution

With the assumptions of the last section, we can compute the values of the moments in equilibrium, by evaluating the integrals with the Bose distribution (11). In particular, we obtain for the energy density the well-known relation to the fourth power of temperature,

$$e = \int \hbar \omega f_{\mathrm{Bose}} \mathrm{d}\mathbf{k} = \int \frac{y \hbar c k}{\exp\left[\frac{\hbar \omega}{k_B T}\right] - 1} \mathrm{d}\mathbf{k} = \frac{4 y \pi^5 k_B^4}{15 c^3 \hbar^3} T^4 = a T^4. \tag{16}$$

By definition, temperature is an equilibrium property. It is customary, though, to extend the above relation to the nonequilibrium case, so that $T = (e/a)^{1/4}$ in all processes. This definition of temperature in nonequilibrium mainly simplifies notation.

We also note that due to the isotropy of the Bose distribution, we have $u_{\langle i_1 \cdots i_n \rangle | \mathrm{Bose}} = 0$ for $n \geq 1$.

2.5 The Callaway model

The right-hand side of the phonon Boltzmann equation is the nonlinear collision term, accounting for resistive and normal processes. In order to simplify the right-hand side, Callaway introduced a simplified model [12], which is analogous to the BGK model in the kinetic theory of classical gases [20]. The Callaway model does not individually resolve phonon interactions but assumes that any phonon interaction increases entropy and thus drives the distribution function toward the equilibrium distribution. Furthermore, since it is the interactions themselves that increase entropy, the rate of increasing entropy depends on the mean free time of phonon interactions, denoted as τ_{N} for normal interactions and τ_{R} for resistive interactions. We simplify the Callaway model by using the gray matter assumption whereby the collision frequencies are assumed to be independent of wave vector or frequency.

The Callaway model states the collision term as

$$S_{\mathrm{N}}(f) + S_{\mathrm{R}}(f) = -\frac{1}{\tau_{\mathrm{N}}}(f - f_{\mathrm{N}}) - \frac{1}{\tau_{\mathrm{R}}}(f - f_{\mathrm{R}}), \tag{17}$$

where f_{N} and f_{R} are suitable equilibrium functions. Both collision terms conserve energy, and the term for normal processes conserves momentum as well, that is,

$$\begin{aligned}
\int \hbar \omega S_{\mathrm{R}}(f) \mathrm{d}\mathbf{k} &= \frac{1}{\tau_{\mathrm{R}}} \int \hbar \omega (f - f_{\mathrm{R}}) \mathrm{d}\mathbf{k} = 0 \\
\int \hbar \omega S_{\mathrm{N}}(f) \mathrm{d}\mathbf{k} &= \frac{1}{\tau_{\mathrm{N}}} \int \hbar \omega (f - f_{\mathrm{N}}) \mathrm{d}\mathbf{k} = 0 \\
\int \hbar k_i S_{\mathrm{N}}(f) \mathrm{d}\mathbf{k} &= \frac{1}{\tau_{\mathrm{N}}} \int \hbar k_i (f - f_{\mathrm{N}}) \mathrm{d}\mathbf{k} = 0
\end{aligned} \tag{18}$$

The equilibrium functions f_{N} and f_{R} are obtained from maximizing entropy (10) under the constraints of given values of those moments that are conserved in interaction, i.e., only energy for resistive processes, and energy

and momentum for normal processes. The Lagrange multipliers of the maximization process are determined from the above conservation requirements. Then, f_{R} is the Bose distribution (11), and f_{N} is the drifting Bose distribution [6,12]

$$f_{\mathrm{N}} = \frac{y}{\exp\left[\hbar\omega\Lambda_e + \hbar k_i \Lambda_i\right] - 1}, \tag{19}$$

where Λ_e and Λ_i are the Lagrange multipliers of the maximization process.

When the deviation from equilibrium is sufficiently small, one can linearize f_{N} around the Bose distribution to obtain, with $\omega = ck$,

$$f_{\mathrm{N}} = f_{\mathrm{Bose}} + \frac{\partial f_{\mathrm{Bose}}}{\partial \frac{\hbar ck}{k_B T}} \left[\hbar ck \left(\Lambda_e - \frac{1}{k_B T}\right) + \hbar k_i \Lambda_i\right]. \tag{20}$$

The Lagrange multipliers follow from the conservation requirements (18) which yield $\Lambda_e = \frac{1}{k_B T}$ and $\Lambda_i = -\frac{45}{16}\frac{\hbar^3 c^5}{y\pi^5 k_B^5 T^5} p_i$ so that

$$f_{\mathrm{N}} = f_{\mathrm{Bose}} - \frac{\partial f_{\mathrm{Bose}}}{\partial k}\frac{3}{4}\frac{cp_i}{aT^4}k_i \ , \tag{21}$$

where $aT^4 = e$ is energy density (16).

2.6 Moment equations

Instead of directly solving the phonon Boltzmann equation to find the distribution function f, the moment method generates a set of moment transport equations by integrating over the phonon Boltzmann equation. Using the assumptions outlined above and applying the gray matter Callaway model, we first find the energy transport equation by multiplying the phonon Boltzmann equation (4) by $\hbar\omega$ and integrating to obtain

$$\frac{\partial e}{\partial t} + c^2 \frac{\partial p_i}{\partial x_i} = 0. \tag{22}$$

Note that the right-hand side of equation (22) must be zero because energy is conserved in phonon collisions, see $(18)_{1,2}$. We recognize, again, $c^2 p_i$ as the phonon energy flux.

The transport equation for momentum is obtained by multiplying the phonon Boltzmann equation with $\hbar k_i$ and subsequent integration, to read

$$\frac{\partial p_i}{\partial t} + \frac{1}{3}\frac{\partial e}{\partial x_i} + c\frac{\partial u_{\langle ij\rangle}}{\partial x_j} = -\frac{1}{\tau_{\mathrm{R}}} p_i. \tag{23}$$

Momentum is conserved in normal processes (see $(18)_3$), but not in resistive processes, which therefore contribute to the production term on the right-hand side. Note the occurrence of the phonon stress tensor $\Pi_{ij} = cu_{ij}$ under the space derivative.

The general moment transport equation for the moments (9) is

$$\frac{\partial u_{\langle i_1 \cdots i_n\rangle}}{\partial t} + c\frac{n}{2n+1}\frac{\partial u_{\langle \langle i \cdots i_{n-1}\rangle}}{\partial x_{i_n\rangle}} + c\frac{\partial u_{\langle i_1 \cdots i_{n+1}\rangle}}{\partial x_{i_{n+1}}} = -\frac{1}{\tau} u_{\langle i \cdots i_n\rangle}, \tag{24}$$

where $\frac{\partial u_{\langle\langle i_1 \cdots i_{n-1}\rangle}}{\partial x_{i_n\rangle}}$ is the trace-free gradient of $u_{\langle i_1 \cdots i_{n-1}\rangle}$ and the overall mean free time τ is defined as

$$\frac{1}{\tau} = \frac{1}{\tau_{\mathrm{R}}} + \frac{1}{\tau_{\mathrm{N}}}. \tag{25}$$

2.7 Closure

Taking moments of the Boltzmann equation generates an infinite set of coupled linear partial differential equations for the macroscopic properties, i.e., the moments, in a solid. For practical applications, the system has to be truncated, so that only a finite number of moments, and the corresponding equations, are considered. We consider a truncated set of moment equations with moments $U_A = \left\{e, u_{\langle i_1 \cdots i_n \rangle} \, (n = 1, \ldots, N)\right\}$. The equation for the highest moment, $u_{\langle i_1 \cdots i_N \rangle}$, contains the moment $u_{\langle i_1 \cdots i_{N+1} \rangle}$ which is not among the variables; hence, a constitutive equation for $u_{\langle i_1 \cdots i_{N+1} \rangle}$ is required to close the system.

The solution to the closure problem was first proposed in kinetic theory by Grad [5] and adapted to phonon kinetic theory later in [6]. The idea is to construct f such that it is a function of only the chosen variables, and of the wave vector, so that the distribution function for closure is of the form $f_{\mathrm{G}} = f\,(\mathbf{k}, U_A\,(\mathbf{x}, t))$. Note that the dependence on space-time is only through the space-time dependence of the variables $U_A\,(\mathbf{x}, t)$. With a proper expression for f_{G}, the higher moment $u_{\langle i_1 \cdots i_{N+1} \rangle}$ can be determined as a function of the lower moments. The function f_{G} will also be needed to construct boundary conditions for the moments.

We follow the approach in [6], where that distribution function is chosen which maximizes phonon entropy in nonequilibrium under constraints of given values for the moments U_A that are considered as variables. The maximization yields

$$f_{\mathrm{G}} = \frac{y}{\exp\left[\hbar c k \Delta_e + \sum_{n=1}^{N} \left\{\Delta_{\langle i_1 \cdots i_n \rangle} \hbar \left(\frac{1}{k}\right)^{n-1} k_{\langle i_1} k_{i_2} \cdots k_{i_n \rangle}\right\}\right] - 1}, \tag{26}$$

where the Lagrange multipliers, Δ_e and $\Delta_{\langle i_1 \cdots i_n \rangle} (n = 1, 2, \ldots, N)$, must be determined from the definition of the moments (9). Again, we consider only small deviations from the equilibrium distribution, which allows us to linearize in the Lagrange multipliers. Then, their computation is straightforward, and the distribution function for closure is

$$f_{\mathrm{G}} = f_{\mathrm{Bose}} - \frac{\partial f_{\mathrm{Bose}}}{\partial k} \sum_{n=1}^{N} \frac{(2n+1)!!}{4n!} \frac{c u_{\langle i_1 \cdots i_n \rangle}}{a T^4} \frac{k_{\langle i_1} \cdots k_{i_n \rangle}}{k^{n-1}}. \tag{27}$$

The required constitutive relation for $u_{\langle i_1 \cdots i_{N+1} \rangle}$ follows from evaluation of (9) with the Grad distribution (27), which gives

$$u_{\langle i_1 \cdots i_{N+1} \rangle} = \int_{-\infty}^{\infty} \hbar \frac{k_{\langle i_1} \cdots k_{i_{N+1} \rangle}}{k^N} f_{\mathrm{G}} \mathrm{d}\mathbf{k} = 0. \tag{28}$$

The closure method thus reduces the number of unknowns to the number of equations. For a more in-depth look into Grad closure, see [21].

3 Boundary conditions

3.1 Boundary condition for the phonon Boltzmann equation

Boundary conditions are required to solve the Boltzmann equation, or the moment equations, for processes in finite systems. We introduce microscopic boundary conditions based on a simple microscopic model for interactions of phonons with the crystal surface. Later, these will be used to create macroscopic boundary conditions for the state variables U_A, i.e., the moments.

Our model for phonon–surface interaction is similar to the well-known Maxwell boundary condition for classical gases [18], which models gas–wall interactions as a mix of specular reflection (exchange of normal momentum only, no exchange of energy) and diffusive reflection (exchange of energy and momentum). It also is a combination of the boundary conditions discussed in [4].

We assume there are three possible interactions between a phonon and the crystal surface: thermalization, specular reflection, and scattering (see Fig. 1). The purpose of this model is to capture the general characteristics of phonon–surface interactions with a model that is simple enough for analytical mathematical modeling. The

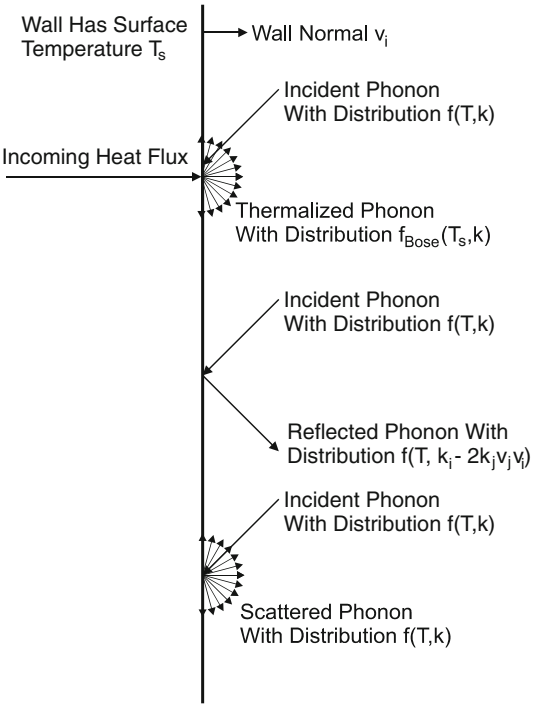

Fig. 1 Phonon interaction processes at the crystal boundary

model is also flexible so that the relative amounts of each type of interaction can be changed to fit experimental results.

For the discussion of thermalization, we recall that phonons may be created or destroyed. Thermalization is a process where (a) incoming phonons are absorbed at the surface and (b) new phonons are emitted from the surface into the crystal. The emitted phonons are in thermal equilibrium with the surface, that is, they leave in a Bose distribution centered on the surface temperature T_s. This process allows for heat transfer across the crystal surface. Note also that quasi-momentum will not be conserved; there will be a phonon radiative pressure on the surface. For instance, when the crystal is exposed to radiation, photons will be absorbed, and emitted, on the outside, while phonons will be absorbed and emitted on the inside. The result is energy transfer across the crystal boundary, as well as normal force and drag due to nonconservation of phonon momentum.

In specular reflection, a phonon strikes the surface and returns to the bulk with a reflection angle equal and opposite to the incidence angle. The phonon energy is conserved, and the momentum normal to the surface is inverted, while tangential momentum is conserved. Phonon energy is conserved; hence, there is no energy transfer across the boundary. Since tangential momentum is conserved, there is no drag associated with this process.

Thermalization and specular reflection are as in the Maxwell mode for classical gases. For increased generality, we also consider isotropic scattering of phonons, where incoming phonons are reflected in a random direction, while keeping their energy. Note that due to the phonon dispersion relation, the magnitude of the phonon momentum is conserved, but not the direction. Since phonon energy is conserved, there is no transfer of energy across the boundary. Phonon momentum changes direction, however, and hence, there is an associated drag on the phonon gas.

To proceed, we define $\bar{f}$ as the particle distribution function for all phonons that have just interacted with the boundary, thus are moving from the boundary into the crystal. The distribution $\bar{f}$ depends on the distribution of incident phonons, f, as well as the surface temperature, T_s, and other parameters describing the proportion of phonons that are thermalized, reflected, or scattered.

We define α as the proportion of phonons that are scattered either isotropically or by specular reflection. Of the scattered phonons, γ are specularly reflected and $1-\gamma$ are scattered. Moreover, β is the relative amount of thermalized phonons. The function $\bar{f}$ then reads

$$\bar{f} = \beta f_{\text{Bose}}\left(T_s, k\right) + \alpha\gamma f\left(k_i - 2k_j v_j v_i\right) + \alpha\frac{(1-\gamma)}{\pi}\frac{1}{c}\int\limits_{n_k v_k<0} c\left(-n_k v_k\right) f\left(k_j\right) \mathrm{d}\mathbf{k}\Omega, \tag{29}$$

where ν_i is the surface normal unit vector pointing into the crystal and $n_i = k_i/k$ is the unit direction vector of the phonons. The first term describes thermalized phonons leaving in the Bose distribution at surface temperature T_s. The second term describes phonons after specular reflection, which have the same distribution $f(k_i)$, albeit with inverted normal momentum. The last term describes the isotropic scattering of incoming phonons. The factor $\alpha\frac{(1-\gamma)}{\pi}$ ensures conservation of the number of scattered phonons [21].

The coefficients α and β cannot be chosen independently from each other. Indeed, in the case of thermal equilibrium, both the incoming and the outgoing distribution functions must be Bose distributions with the same temperature $T_\mathrm{s} = T$, in which case (29) assumes the form

$$f_\mathrm{Bose}(T_\mathrm{s}, k) = \beta f_\mathrm{Bose}(T_\mathrm{s}, k) + \alpha\gamma f_\mathrm{Bose}(T_\mathrm{s}, k) + \alpha\frac{(1-\gamma)}{\pi}\frac{1}{c}\int\limits_{n_k\nu_k<0} c(-n_k\nu_k)\, f_\mathrm{Bose}(T_\mathrm{s}, k)\,\mathrm{d}\Omega. \quad (30)$$

Since f_Bose is isotropic, the integral can be solved easily, and the above yields

$$\beta = 1 - \alpha. \quad (31)$$

The parameters α, β, and γ describe, in terms of probabilities, how individual phonons interact with the surface. We assume that a phonon that interacts with the surface is not at the same time interacting with other phonons, which indeed would be rather unlikely. Then, the surface interaction is not affected by the state of the phonon gas in the bulk; hence, the coefficients α, β, and γ are properties of the surface alone. It follows that the above relation between α and β, which was derived for equilibrium, is valid also in nonequilibrium.

To summarize this section, the distribution function f_B directly at the crystal boundary is the bulk distribution $f(\mathbf{x}, t, \mathbf{k})$ for incoming phonons ($\nu_i n_i < 0$), and it is the distribution function $\bar{f}(\mathbf{x}, t, \mathbf{k})$ as given in (29) for outgoing phonons; we write

$$f_\mathrm{B} = \begin{cases} f(\mathbf{x}, t, \mathbf{k}), & \nu_i n_i < 0 \\ \bar{f}(\mathbf{x}, t, \mathbf{k}), & \nu_i n_i > 0 \end{cases} \quad (32)$$

3.2 Boundary conditions for moments

We proceed with finding boundary conditions for the moment equations from the boundary condition for the phonon Boltzmann equation. Thus, from now on, we assume that the phonons in the bulk are described by the Grad distribution, that is, we set $f = f_\mathrm{G}$. The distribution function directly at the crystal boundary, f_B in Eq. (32), must now be evaluated with f_G.

Macroscopic boundary conditions for the moments are obtained from the requirement that normal fluxes of moments formed with f_B and with the bulk distribution f agree; this idea is well known in classical kinetic theory [5,22]. The resulting requirement reads

$$\int k n_{i_1}\cdots n_{i_n} c n_k \nu_k f_\mathrm{B}\,\mathrm{d}\mathbf{k} = \int k n_{i_1}\cdots n_{i_n} c n_k \nu_k f\,\mathrm{d}\mathbf{k}; \quad (33)$$

where n runs from 0 to N. Note that we consider the fluxes of full moments, not of the trace-free parts. Since f and f_B agree for incident particles, this simplifies to

$$\int\limits_{n_k\nu_k>0} k n_{i_1}\cdots n_{i_n} c n_k \nu_k \bar{f}\,\mathrm{d}\mathbf{k} = \int\limits_{n_k\nu_k>0} k n_{i_1}\cdots n_{i_n} c n_k \nu_k f\,\mathrm{d}\mathbf{k}. \quad (34)$$

To proceed, we consider a frame where the normal on the boundary points in 3-direction, such that the phonon direction vector is $n_k = \{\tau_A, \nu\}_k$ with the normal component $\nu = n_k\nu_k = \cos\theta$ and the tangential vector $\tau_A = \{\sin\theta\cos\phi, \sin\theta\sin\phi\}_A$. In this notation, capital indices denote 2-D tangential components. Accordingly, we replace $n_{i_1}\cdots n_{i_n} \Longrightarrow \tau_{A_1}\cdots\tau_{A_r}\nu^{n-r}$, which yields the boundary conditions as

$$\int\limits_{n_k\nu_k>0} k\tau_{A_1}\cdots\tau_{A_r}\nu^{n-r+1}\bar{f}\,\mathrm{d}\mathbf{k} = \int\limits_{n_k\nu_k>0} k\tau_{A_1}\cdots\tau_{A_r}\nu^{n-r+1} f\,\mathrm{d}\mathbf{k}; \quad (35)$$

here, $r \in (0, n)$ and $n \in (0, N)$.

Equation (35) provides more equations than required. In [5] Grad provided further restriction on the conditions by considering the special case where there is only specular reflection (i.e., $\alpha = 1,\ \beta = 1-\alpha = 0,\ \gamma = 1$). Then, with (29), Eq. (35) reduces to

$$\int_{\nu>0} k\tau_{A_1}\cdots\tau_{A_r}\nu^{n-r+1} f(-\nu)\ \mathrm{d}\mathbf{k} = \int_{\nu>0} k\tau_{A_1}\cdots\tau_{A_r}\nu^{n-r+1} f(\nu)\ \mathrm{d}\mathbf{k} \tag{36}$$

where $f(-\nu)$ is the distribution function with inverted normal direction, since $k_i - 2k_j\nu_j\nu_i = k\left(n_i - 2n_j\nu_j\nu_i\right) = k\{\tau_A, -\nu\}$. Distinguishing between even and odd values of $(n-r)$, this can be written as

$$\begin{aligned} 0 &= \int k\tau_{A_1}\cdots\tau_{A_r}\nu^{n-r+1} f(\nu)\ \mathrm{d}\mathbf{k} && (n-r)\ \text{even} \\ 0 &= \int_{\nu>0} k\tau_{A_1}\cdots\tau_{A_r}\nu^{n-r+1}\left(f(\nu) - f(-\nu)\right)\mathrm{d}\mathbf{k} && (n-r)\ \text{odd} \end{aligned} \tag{37}$$

Grad argued that if f is even in ν, and $(n-r)$ is odd, the condition is just an identity and therefore provides no information and must be rejected. Grad argued further that if a condition has to be rejected in a special case, it must be rejected in the general case as well. Hence, only those conditions (35) where $(n-r)$ is even should be considered.

Details for the evaluation are given in "Appendices A and B," where we give only the final expression, which reads, with $e = aT^4$ and $e_s = aT_s^4$,

$$\begin{aligned} &\left[(1-\alpha)(e_s - e) + \alpha(1-\gamma)\sum_{m=1}^{N}\vartheta_m c u_{\langle\nu\cdots\nu\rangle|m}\right]\hat{\sigma}_r^n\delta_{\{A_1A_2\cdots A_r\}} \\ &-\sum_{m=1}^{N}\sum_{\substack{s=0 \\ r+s\ \text{even}}}^{m}\left[1-(-1)^{m-s}\alpha\gamma\right]\frac{(2m+1)!!}{s!\,(m-s)!}c u_{\langle B_1\cdots B_s\nu\cdots\nu\rangle|m}\hat{\sigma}_{r+s}^{n+m}\delta_{\{A_1A_2\cdots A_rB_1B_2\cdots B_s\}} = 0,\ (n-r)\ \text{even} \end{aligned} \tag{38}$$

The notation is respective to the boundary considered, capital indices refer to tangential directions, while indices ν refer to the normal direction. Thus, $u_{\langle B_1\cdots B_s\nu\cdots\nu\rangle|m}$ denotes the s-fold tangential and $(m-s)$-fold normal component of the moment with m indices. The general unit tensor $\delta_{\{A_1\cdots A_n\}}$ is defined as the sum of all Kronecker deltas in a fully symmetric tensor (see Eq. (82) in "Appendix A").

4 Specific systems of equations and boundary conditions

The transport equations are presented here in their general form for the 4, 9, 16, and 25 moment equations along with their boundary conditions. For better readability, we introduce the variables energy density $e = cu = aT^4$, phonon momentum $p_i = u_i$, reduced phonon stress tensor $N_{\langle ij\rangle} = u_{\langle ij\rangle} = \Pi_{\langle ij\rangle}/c$, and the higher moments $M_{\langle ijk\rangle} = u_{\langle ijk\rangle}$, and $R_{\langle ijkl\rangle} = u_{\langle ijkl\rangle}$.

4.1 25-Moment equations ($N = 4$)

The largest system we shall consider here is the 25-moment system, for the variables $\{e, p_i, N_{\langle ij\rangle}, M_{\langle ijk\rangle}, R_{\langle ijkl\rangle}\}$. Smaller systems are obtained from removing terms from these, as will be pointed out below. The moment equations for the 25-moment case read

$$
\begin{aligned}
\frac{\partial e}{\partial t} + c^2 \frac{\partial p_i}{\partial x_i} &= 0 \\
\frac{\partial p_i}{\partial t} + \frac{1}{3}\frac{\partial e}{\partial x_i} + c\frac{\partial N_{\langle ik\rangle}}{\partial x_k} &= -\frac{1}{\tau_{\mathrm{R}}} p_i \\
\frac{\partial N_{\langle ij\rangle}}{\partial t} + \frac{2}{5} c \frac{\partial p_{\langle i}}{\partial x_{j\rangle}} + c\frac{\partial M_{\langle ijk\rangle}}{\partial x_k} &= -\frac{1}{\tau} N_{\langle ij\rangle} \\
\frac{\partial M_{\langle ijk\rangle}}{\partial t} + \frac{3}{7} c \frac{\partial N_{\langle\langle ij\rangle}}{\partial x_{k\rangle}} + c\frac{\partial R_{\langle ijkl\rangle}}{\partial x_l} &= -\frac{1}{\tau} M_{\langle ijk\rangle} \\
\frac{\partial R_{\langle ijkl\rangle}}{\partial t} + \frac{4}{9} c \frac{\partial M_{\langle\langle ijk\rangle}}{\partial x_{l\rangle}} &= -\frac{1}{\tau} R_{\langle ijkl\rangle}
\end{aligned}
\tag{39}
$$

The first equation is the energy balance, with the energy flux $c^2 p_i$, and the second is the momentum balance, which can also be interpreted as balance equation for the energy flux.

The required boundary conditions are obtained from (38) for the following choices of n and r:

For $n = r = 0$, we find

$$
p_\nu = -\frac{1}{2}\frac{1-\alpha}{1+\alpha}\left[\frac{e - e_s}{c} + \frac{15}{8} N_{\langle \nu\nu\rangle} - \frac{105}{64} R_{\langle \nu\nu\nu\nu\rangle}\right]. \tag{40}
$$

This relation is analogous to the temperature jump boundary condition in rarefied gases [22]. The normal energy flux $c^2 p_\nu$ is proportional to the energy jump $e_s - e$ and affected by higher moments as well. Notably, the energy flux is proportional to the amount $(1-\alpha)$ of thermalization processes. This reflects that in specular reflection and isotropic scattering, phonon energy is conserved; in particular, when no thermalization occurs, i.e., for $\alpha = 1$, the boundary is adiabatic ($p_\nu = 0$).

For $n = r = 1$, we find

$$
N_{\langle A\nu\rangle} = -\frac{3}{8}\frac{1-\alpha\gamma}{1+\alpha\gamma}\left[p_A + \frac{35}{12} M_{\langle A\nu\nu\rangle}\right] + \frac{3}{2} R_{\langle A\nu\nu\nu\rangle}. \tag{41}
$$

This relation is analogous to the slip condition in rarefied gases [22]. The shear stress at the crystal surface is proportional to the tangential momentum and affected by higher moments as well. Note that $(1-\alpha\gamma)$ is the relative amount of thermalization and isotropic scattering processes.

The other boundary conditions relate higher moments. In particular, we find:

For $n = 2, r = 0$, after using (40) to eliminate $e_s - e$,

$$
M_{\langle \nu\nu\nu\rangle} = -\frac{1}{10} p_\nu - \frac{15}{32}\frac{1-\alpha\gamma}{1+\alpha\gamma}\left[N_{\langle \nu\nu\rangle} + \frac{35}{16} R_{\langle \nu\nu\nu\nu\rangle}\right]; \tag{42}
$$

for $n = 2, r = 2$, after using (40, 42),

$$
M_{\langle AB\nu\rangle} + \frac{1}{2} M_{\langle \nu\nu\nu\rangle}\delta_{AB} = -\frac{(1-\alpha\gamma)}{(1+\alpha\gamma)}\frac{5}{16}\left[N_{\langle AB\rangle} + \frac{1}{2} N_{\langle \nu\nu\rangle}\delta_{AB} + \frac{63}{16}\left(R_{\langle \nu\nu AB\rangle} + \frac{1}{2} R_{\langle \nu\nu\nu\nu\rangle}\delta_{AB}\right)\right]; \tag{43}
$$

note that the 2-trace of this relation is an identity, since, e.g., $N_{\langle AB\rangle}\delta_{AB} = -N_{\langle \nu\nu\rangle}$ and $\delta_{AB}\delta_{AB} = 2$.

For $n = 3, r = 1$,

$$
R_{\langle \nu\nu\nu A\rangle} = \frac{1-\alpha\gamma}{1+\alpha\gamma}\frac{3}{4}\left[p_A + \frac{105}{16} M_{\langle \nu\nu A\rangle}\right] + \frac{18}{7} N_{\langle \nu A\rangle}, \tag{44}
$$

for $n = 3, r = 3$, with (44),

$$
R_{\langle ABC\nu\rangle} = \frac{1-\alpha\gamma}{1+\alpha\gamma}\frac{3}{16}\left[p_{\langle A}\delta_{BC\rangle} + \frac{175}{16} M_{\langle \nu\nu\langle A\rangle}\delta_{BC\rangle} - \frac{35}{24} M_{\langle ABC\rangle}\right] + \frac{6}{7} N_{\langle \nu\langle A\rangle}\delta_{BC\rangle} \tag{45}
$$

Equation sets with fewer moments are obtained from the above by removing moments and their equations and boundary conditions. The resulting equations will be discussed next.

4.2 4-Moment equations ($N = 1$)

The simplest moment system has the variables $\{e, p_i\}$ with the transport equations

$$\begin{aligned} \frac{\partial e}{\partial t} + c^2 \frac{\partial p_i}{\partial x_i} &= 0 \\ \frac{\partial p_i}{\partial t} + \frac{1}{3}\frac{\partial e}{\partial x_i} &= -\frac{1}{\tau_{\mathrm{R}}} p_i . \end{aligned} \tag{46}$$

There is only one boundary condition,

$$p_\nu = -\frac{1}{2}\frac{1-\alpha}{1+\alpha}\left[\frac{e-e_s}{c}\right]. \tag{47}$$

The Knudsen number for resistive processes is defined as

$$\mathrm{Kn}_{\mathrm{R}} = \frac{\tau_{\mathrm{R}}}{L/c}, \tag{48}$$

where L is a relevant length scale of the process or device. For small Kn_{R}, the equations can be simplified by a Chapman–Enskog expansion. We omit all details on the expansion and just state that the momentum balance reduces to Fourier's law, which we write for the energy flux $c^2 p_i$ as

$$c^2 p_i = -\frac{c^2 \tau_{\mathrm{R}}}{3}\frac{\partial e}{\partial x_i} = -\frac{4}{3} c^2 \tau_{\mathrm{R}} a T^3 \frac{\partial T}{\partial x_i} = -\kappa\,(T)\,\frac{\partial T}{\partial x_i}. \tag{49}$$

Here, $\kappa\,(T) = \frac{4}{3} c^2 \tau_{\mathrm{R}} a T^3$ is the heat conductivity; its measurement allows the determination of the relaxation time τ_{R} as a function of temperature.

The full 4-moment system—with the time derivative $\frac{\partial p_i}{\partial t}$—would be relevant when $\frac{1}{\tau_{\mathrm{R}}}$ is finite, but $\frac{1}{\tau} = \frac{1}{\tau_{\mathrm{R}}} + \frac{1}{\tau_{\mathrm{N}}}$ goes to infinity, which happens for $\tau_{\mathrm{N}} \to 0$. In this case, all higher moments $u_{\langle i_1 \cdots i_n \rangle} (n \geq 2)$ must vanish, since else the production terms $u_{\langle i_1 \cdots i_n \rangle}/\tau$ in the moment equations (24) become infinite. To be more specific, the requirement is vanishing overall Knudsen number $\mathrm{Kn} = \frac{\tau}{L/c}$, and finite Knudsen number Kn_{R}, or a rather large rate of normal processes and low rate of resistive processes. The resulting equations describe second sound, that is, wavelike heat transfer, with wave speed $v_{II} = \frac{c}{\sqrt{3}}$ [6]. It seems that no physical system exits, where the relevant conditions are met [6].

4.3 9-Moment equations ($N = 2$)

An often discussed system [6,8] is the 9-moment case, with the variables $\left\{e, p_i, N_{\langle ij \rangle}\right\}$. The transport equations are

$$\begin{aligned} \frac{\partial e}{\partial t} + c^2 \frac{\partial p_i}{\partial x_i} &= 0, \\ \frac{\partial p_i}{\partial t} + \frac{1}{3}\frac{\partial e}{\partial x_i} + c\frac{\partial N_{\langle ik \rangle}}{\partial x_k} &= -\frac{1}{\tau_{\mathrm{R}}} p_i , \\ \frac{\partial N_{\langle ij \rangle}}{\partial t} + \frac{2}{5} c \frac{\partial p_{\langle i}}{\partial x_{j \rangle}} &= -\frac{1}{\tau} N_{\langle ij \rangle}, \end{aligned} \tag{50}$$

with the boundary conditions

$$\begin{aligned} p_\nu &= -\frac{1}{2}\frac{1-\alpha}{1+\alpha}\left[\frac{e-e_s}{c} + \frac{15}{8} N_{\langle \nu\nu \rangle}\right], \\ N_{\langle A\nu \rangle} &= -\frac{3}{8}\frac{1-\alpha\gamma}{1+\alpha\gamma} p_A . \end{aligned} \tag{51}$$

This system describes phonon hydrodynamics including the effects of the phonon stress tensor $\Pi_{\langle ij \rangle} = c N_{\langle ij \rangle}$; it was used successfully to describe the measurements of second sound in [6]. The boundary conditions

describe the energy (or temperature) jump at the boundary due to the energy flow crossing the boundary, and the tangential slip of the phonon gas due to shear stress.

In case that the overall Knudsen number $\mathrm{Kn} = \frac{\tau}{L/c}$ is small, but the resistive Knudsen number $\mathrm{Kn_R}$ is not small, the equation for $N_{\langle ij\rangle}$ can be reduced by means of a Chapman–Enskog expansion in Kn, which yields a Navier–Stokes-like law for the stress tensor [6],

$$N_{\langle ij\rangle} = -\frac{2}{5}\tau c \frac{\partial p_{\langle i}}{\partial x_{j\rangle}}. \tag{52}$$

When this is inserted into the momentum equation, we obtain a system very similar to the well-known Guyer–Krumhansl equations for phonon hydrodynamics [10,11],

$$\frac{\partial e}{\partial t} + c^2 \frac{\partial p_i}{\partial x_i} = 0 \tag{53}$$

$$\frac{\partial p_i}{\partial t} + \frac{1}{3}\frac{\partial e}{\partial x_i} - \frac{1}{5}\tau c^2 \left(\frac{\partial^2 p_i}{\partial x_k \partial x_k} + \frac{1}{3}\frac{\partial^2 p_k}{\partial x_i \partial x_k} \right) = -\frac{1}{\tau_\mathrm{R}} p_i. \tag{54}$$

The difference to the original Guyer–Krumhansl equations is the factor on the derivative $\frac{\partial^2 p_k}{\partial x_i \partial x_k}$, which is $\left(\frac{1}{3}\right)$ in our equations, while Guyer and Krumhansl report the factor 2. This difference is due to the occurrence of a bulk viscosity term in the Guyer–Krumhansl equations, which appears as a result of having frequency-dependent relaxation times in the Callaway model. The boundary conditions for this set of equations follow from (51) with the expression (52) for $N_{\langle ij\rangle}$; they read

$$\begin{aligned} p_\nu &= -\frac{1}{2}\frac{1-\alpha}{1+\alpha}\left[\frac{e-e_s}{c} - \tau c \frac{1}{4}\left(2\frac{\partial p_\nu}{\partial x_\nu} - \frac{\partial p_A}{\partial x_A} \right) \right], \\ p_A &= \frac{8}{15}\frac{1+\alpha\gamma}{1-\alpha\gamma}\tau c \left(\frac{\partial p_A}{\partial x_\nu} + \frac{\partial p_\nu}{\partial x_A} \right). \end{aligned} \tag{55}$$

The slip condition was used in [7], however, without the term $\frac{\partial p_\nu}{\partial x_A}$ that describes slip due to a gradient of normal heat flux along the boundary. A term like this does not appear in classical gas kinetic theory, since there the gas velocity appears instead of momentum, and the normal velocity must vanish at an impermeable wall. The term in question does vanish only for an adiabatic boundary, where $p_\nu = 0$ so that the slip condition reduces to $p_A = \frac{1+\alpha\gamma}{1-\alpha\gamma}\frac{8}{15}\tau c \frac{\partial p_A}{\partial x_\nu}$.

4.4 16-Moment equations ($N = 3$)

When the flux of the stress tensor is considered as another variable, the set of variables is $\{e, p_i, N_{\langle ij\rangle}, M_{\langle ijk\rangle}\}$ with the transport equations

$$\begin{aligned} \frac{\partial e}{\partial t} + c^2 \frac{\partial p_i}{\partial x_i} &= 0, \\ \frac{\partial p_i}{\partial t} + \frac{1}{3}\frac{\partial e}{\partial x_i} + c\frac{\partial N_{\langle ik\rangle}}{\partial x_k} &= -\frac{1}{\tau_\mathrm{R}} p_i, \\ \frac{\partial N_{\langle ij\rangle}}{\partial t} + \frac{2}{5}c\frac{\partial p_{\langle i}}{\partial x_{j\rangle}} + c\frac{\partial M_{\langle ijk\rangle}}{\partial x_k} &= -\frac{1}{\tau} N_{\langle ij\rangle}, \\ \frac{\partial M_{\langle ijk\rangle}}{\partial t} + \frac{3}{7}c\frac{\partial N_{\langle\langle ij\rangle}}{\partial x_{k\rangle}} &= -\frac{1}{\tau} M_{\langle ijk\rangle}, \end{aligned} \tag{56}$$

and the boundary conditions

$$\begin{aligned} p_\nu &= -\frac{1-\alpha}{1+\alpha}\frac{1}{2}\left[\frac{e-e_s}{c} + \frac{15}{8} N_{\langle\nu\nu\rangle} \right] \\ N_{\langle\nu A\rangle} &= -\frac{1-\alpha\gamma}{1+\alpha\gamma}\frac{3}{8}\left[p_A + \frac{35}{12} M_{\langle\nu\nu A\rangle} \right] \end{aligned}$$

$$M_{\langle\nu\nu\nu\rangle} = -\frac{1}{10}p_\nu - \frac{15}{32}\frac{1-\alpha\gamma}{1+\alpha\gamma}N_{\langle\nu\nu\rangle}$$
$$M_{\langle AB\nu\rangle} + \frac{1}{2}M_{\langle\nu\nu\nu\rangle}\delta_{AB} = -\frac{(1-\alpha\gamma)}{(1+\alpha\gamma)}\frac{5}{16}\left[N_{\langle AB\rangle} + \frac{1}{2}N_{\langle\nu\nu\rangle}\delta_{AB}\right] \tag{57}$$

We note the occurrence of the term $\frac{35}{12}M_{\langle\nu\nu A\rangle}$ in the slip boundary condition $(57)_2$. By means of the Chapman–Enskog expansion, this term can be related to second-order derivatives of phonon momentum. Indeed, we have performed a similar analysis in kinetic theory of classical gases [23], where the boundary conditions of extended moment equations were reduced to second-order boundary conditions for the Navier–Stokes equations as discussed in [24]. The corresponding treatment of the above equations will yield second-order boundary conditions for the Guyer–Krumhansl equations (53, 54); for space reasons, we shall not go into details. Hence, this boundary condition can be used to support the second-order boundary condition suggested and evaluated in detail in [8,9].

5 Analytical solutions in simple geometries

The transport equations for phonons will now be used to solve specific problems. With the current assumptions, the set of equations are linear ordinary differential equations with linear boundary conditions. The equations can be used to analytically solve some simple problems with specific geometries. Below, we present solutions for one-dimensional heat transfer and phonon Poiseuille flow. We shall not aim at aligning the equations with actual measurements, but rather study the general behavior of the various sets of equations in dependence of the modeling parameters α, β, γ, $\mathrm{Kn_R}$, and Kn.

5.1 One-dimensional heat transfer

We consider one-dimensional steady heat transfer in the x-direction in a crystal of length L and infinite extension in the other directions. Hence, there are no effects of boundaries along the flow; indeed, the effect of these will be considered in the Poiseuille flow problem. The temperatures at $x = -\frac{L}{2}$ and $x = \frac{L}{2}$ are controlled, which correspond to prescribed values of the surface energy $e_s\left(\pm\frac{L}{2}\right)$. We shall evaluate the problem with the 4, 9, 16, and 25 moment equations presented in the previous section and assume constant relaxation times.

In this 1-D case, at steady state, the equations can be simplified considerably. It is convenient to introduce dimensionless variables and coordinates, such that $L = 1$ and $c = 1$, and we use the average energy $\bar{e} = \frac{1}{2}\left(e_s\left(-\frac{L}{2}\right) + e_s\left(\frac{L}{2}\right)\right)$ to nondimensionalize energy and the other moments. With $p = p_x$, $N = N_{\langle xx\rangle}$, etc., the dimensionless 25-moment equations reduce to

$$\begin{aligned}
\frac{\partial p}{\partial x} &= 0\\
\frac{1}{3}\frac{\partial e}{\partial x} + \frac{\partial N}{\partial x} &= -\frac{1}{\mathrm{Kn_R}}p\\
\frac{4}{15}\frac{\partial p}{\partial x} + \frac{\partial M}{\partial x} &= -\frac{1}{\mathrm{Kn}}N\\
\frac{9}{35}\frac{\partial N}{\partial x} + \frac{\partial R}{\partial x} &= -\frac{1}{\mathrm{Kn}}M\\
\frac{16}{63}\frac{\partial M}{\partial x} &= -\frac{1}{\mathrm{Kn}}R
\end{aligned} \tag{58}$$

With the dimensionless energies prescribed at the crystal boundaries denoted as $E_\pm = e_s\left(\pm\frac{1}{2}\right)$, the boundary conditions at $x = \pm\frac{1}{2}$ are:

$$\begin{aligned}
p &= -\nu\frac{1}{2}\frac{1-\alpha}{1+\alpha}\left[(e - E_\pm) + \frac{15}{8}N - \frac{105}{64}R\right],\\
M &= -\frac{1}{10}p - \nu\frac{15}{32}\frac{1-\alpha\gamma}{1+\alpha\gamma}\left[N + \frac{35}{16}R\right];
\end{aligned} \tag{59}$$

with the normal factor $\nu = \mp 1$ to account for the fact that at $x = -\frac{1}{2}$ the surface normal points into positive direction, while at $x = \frac{1}{2}$ it points into negative direction. For the 4-, 9-, and 16-moment cases, the above equations and boundary conditions must be reduced in an obvious manner.

According to $(58)_1$, the energy flux is constant, $p = \text{const}$. The integration of the momentum balance then gives

$$\frac{1}{3}e + N = C_1 - \frac{px}{\mathrm{Kn_R}} \tag{60}$$

where C_1 is a constant of integration. This equation holds for all moment systems (but with $N = 0$ for the 4-moment case).

We first consider the cases with 4 and 9 moments. Due to geometry, shear stress vanishes in the 9-field case, $N = 0$, and hence, 4- and 9-field theories give the same result. The explicit solutions for energy and energy flux read

$$e = \frac{1}{2}(E_+ + E_-) + \frac{E_+ - E_-}{1 + \frac{4}{3}\mathrm{Kn_R}\frac{1+\alpha}{1-\alpha}}x, \tag{61}$$

$$p = \frac{\mathrm{Kn_R}}{3}\frac{E_+ - E_-}{1 + \frac{4}{3}\mathrm{Kn_R}\frac{1+\alpha}{1-\alpha}}. \tag{62}$$

Accordingly, the energy is linear in space, and, of course, the energy flux is constant. Note that since $e = aT^4$, the temperature curve is nonlinear.

In the 16-moment case, the equations for N and M can be combined into

$$N = \frac{9}{35}\mathrm{Kn2}\frac{\partial^2 N}{\partial x^2}, \qquad M = -\mathrm{Kn}\frac{9}{35}\frac{\partial N}{\partial x} \tag{63}$$

which is easy to solve for stress,

$$N = C_2 \cosh\sqrt{\frac{35}{9}}\frac{x}{\mathrm{Kn}} + C_3 \sinh\sqrt{\frac{35}{9}}\frac{x}{\mathrm{Kn}}; \tag{64}$$

M then follows from differentiation. With this, the general solution for energy is

$$e = 3C_1 - \frac{3px}{\mathrm{Kn_R}} - 3\left(C_2 \cosh\sqrt{\frac{35}{9}}\frac{x}{\mathrm{Kn}} + C_3 \sinh\sqrt{\frac{35}{9}}\frac{x}{\mathrm{Kn}}\right), \tag{65}$$

where $\{p, C_1, C_2C_3\}$ are constants of integration that must be determined from the boundary conditions (59) (with $R = 0$). We shall not show the resulting expressions to save space. Due to symmetry of the problem, we find $C_2 = 0$.

For the 25-moment case, the equations for N, M, and R can be reduced to read

$$\frac{23}{45}\mathrm{Kn}^2\frac{\partial^2 N}{\partial x^2} = N, \qquad M = -\frac{23}{45}\mathrm{Kn}\frac{\partial N}{\partial x}, \qquad R = \frac{16}{63}N \tag{66}$$

Again, the stress N is obtained by integration,

$$N = C_2 \cosh\sqrt{\frac{45}{23}}\frac{x}{\mathrm{Kn}} + C_3 \sinh\sqrt{\frac{45}{23}}\frac{x}{\mathrm{Kn}} \tag{67}$$

and with this, M and R can be determined easily. The solution for energy reads

$$e = 3C_1 - \frac{3px}{\mathrm{Kn_R}} - 3\left(C_2 \cosh\sqrt{\frac{45}{23}}\frac{x}{\mathrm{Kn}} + C_3 \sinh\sqrt{\frac{45}{23}}\frac{x}{\mathrm{Kn}}\right). \tag{68}$$

Again, $\{p, C_1, C_2C_3\}$ are constants of integration that must be determined from the boundary conditions (59); because of symmetry $C_2 = 0$, other results are not shown.

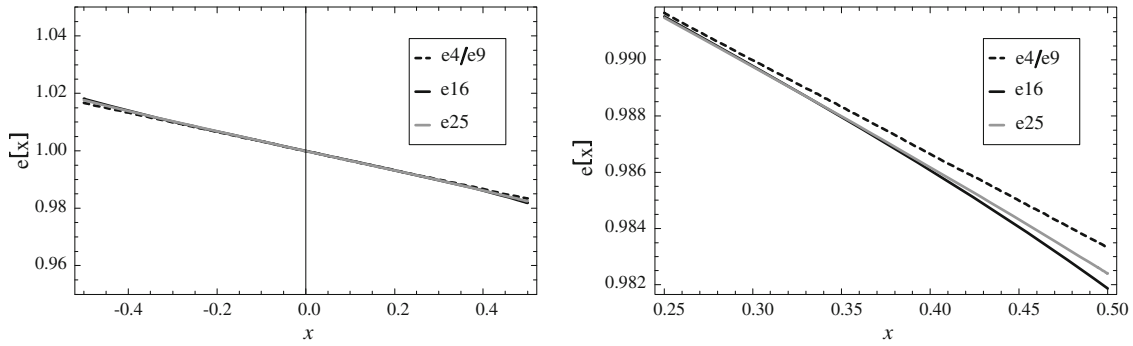

Fig. 2 Energy profiles for solutions of the 4/9-, 16-, and 25-moment equations for $\mathrm{Kn} = 0.25$, $\mathrm{Kn_R} = 0.5$, $\alpha = 0.5$, $\gamma = 0$. Energy values at the boundaries are $E_- = 1.05$ and $E_+ = 0.95$. The *right figure* shows a closer look at the curves in the vicinity of the right boundary

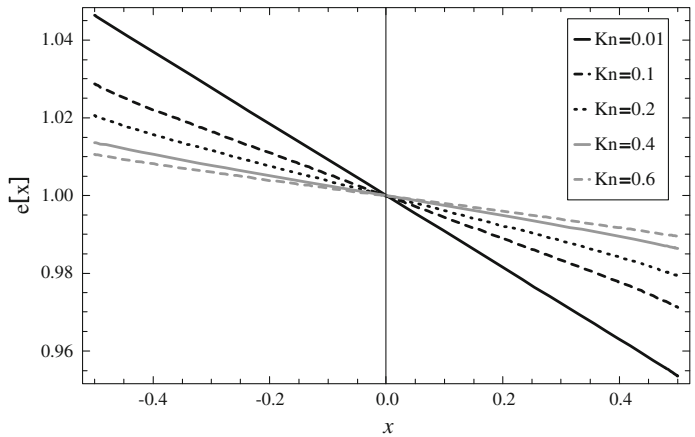

Fig. 3 The 16-moment solution for heat conduction between parallel surfaces with varying Knudsen number. In all cases, $E_- = 1.05$, $E_+ = 0.95$, $\mathrm{Kn_R} = 2\mathrm{Kn}$, $\alpha = 0.5$ and $\gamma = 0$

While the 4- and 9-moment cases give the simple linear function (61) for the energy, the 16- and 25-moment systems in addition exhibit a term $C_3 \sinh \frac{\lambda x}{\mathrm{Kn}}$ (with $\lambda = \sqrt{\frac{35}{9}}$ and $\lambda = \sqrt{\frac{45}{23}}$, respectively). This additional term describes Knudsen boundary layers, as discussed in [25].

To highlight the differences in the solutions, Fig. 2 shows the energy profiles of the 4/9-, 16-, and 25-moment equations for $\mathrm{Kn} = 0.25$, $\mathrm{Kn_R} = 0.5$, $\alpha = 0.5$, $\gamma = 0$, and $E_- = 1.05$, $E_+ = 0.95$. As can be seen in the figure, the jump at the boundary is the dominant effect in the solution as opposed to the Knudsen layers. Due to the Knudsen layers, the curves differ in the vicinity of the boundary, but the differences are small. In the bulk, which is sufficiently away from the boundary, the curves agree well. The dimensionless energy flux p is very close for all three solutions, with the numerical values of $\{0.00556, 0.00549, 0.00549\}$ for 4/9, 16, and 25 moments, respectively.

Obviously, the solution is dependent on a number of parameters, i.e., the Knudsen numbers $\mathrm{Kn_R}$ and Kn and the boundary parameters α and γ. Figure 3 shows the 16-moment solution for a variety of Knudsen numbers. As Knudsen number increases, the temperature jump increases as well. The Knudsen layer contributes to the result, but cannot be resolved by the eye.

Moreover, the temperature jump is affected by the proportion of phonons that bounce off the wall without energy change (α) and thermalize at the wall ($1 - \alpha$). Figure 4 shows the 16-moment solution for $\mathrm{Kn} = 0.1$ for various values of α. When α is small, most phonons thermalize at the wall, allowing more effective heat transfer, and therefore, the temperature jump is smaller. As α grows, more phonons are reflected, so that less phonons contribute to the heat transfer at the boundary, and heat transfer is inhibited. When $\alpha = 1$, the wall is adiabatic and no heat transfer occurs into the bulk phonon gas, which therefore has homogeneous temperature.

The overall heat flux through the domain can be determined and compared to what would be expected by Fourier's law without jump, $p_F = \frac{\mathrm{Kn_R}}{3}(E_+ - E_-)$, which is the appropriate value for systems with small

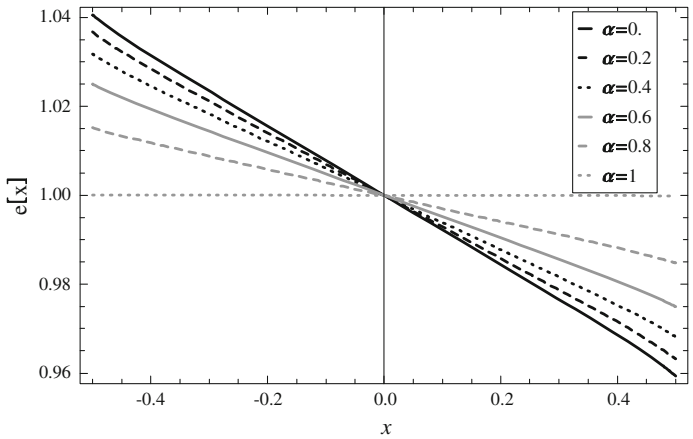

Fig. 4 The 16-moment solution for heat conduction between parallel surfaces for various values of α. In all cases, $\mathrm{Kn_R} = 2\mathrm{Kn}$, $\mathrm{Kn} = 0.1$ and $\gamma = 0$

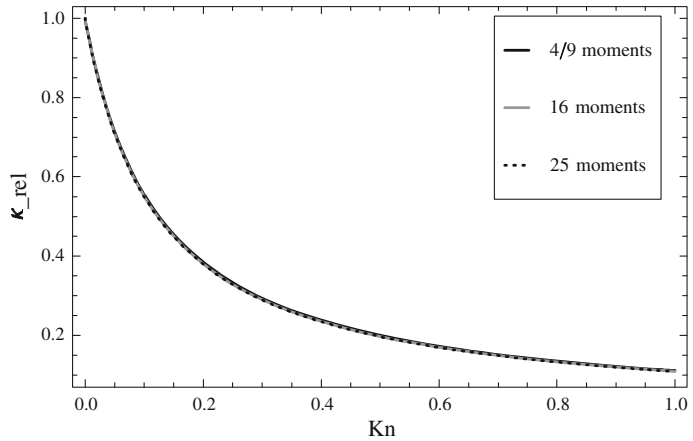

Fig. 5 Relative heat conductivity κ_{rel} for the 4/9-, 16-, and 25-moment equations compared to Fourier's law without jump for varying Knudsen number; $\mathrm{Kn_R} = 2\mathrm{Kn}$, $\alpha = 0.5$, and $\gamma = 0$

Knudsen numbers. For larger Knudsen numbers, the heat flux will be proportional to the energy difference $(E_+ - E_-)$, but with a different factor, i.e., $p \sim (E_+ - E_-)$. This can be used to determine a relative heat conductivity for a system with larger Knudsen number as

$$\kappa_{\mathrm{rel}} = \frac{p}{p_F} = \frac{3p}{\mathrm{Kn_R}\,(E_+ - E_-)}. \tag{69}$$

Figure 5 shows the relative heat conductivity κ_{rel} for the 4/9-, 16-, and 25-moment equations. There is no visible difference between the theories; they all give a decreasing relative conductivity for increasing Knudsen number. The main reason for the decrease is the increasing temperature jump at the boundaries. Obviously, the exact results depend on the parameter in the models, in particular the relaxation times τ and τ_{R} (or the respective Knudsen numbers Kn and $\mathrm{Kn_R}$), and the coefficients α and γ that appear in the boundary conditions. These must be determined from careful experiments, or through first-principle consideration of the material, and the crystal boundaries. The goal of this paper is general exploration of moment equations with boundary conditions, and we shall not attempt to determine realistic values for the parameters.

5.2 Heat transfer across a junction

Many microdevices have a sandwich-like structure. Each boundary between different materials, or different grains of the same material, is an obstacle for phonons and thus inhibits heat transfer. For the description of

this, our model of boundary conditions must be applied at each interface. We note that in its present form, the model does not allow for phonon transmission across the interface, as it would occur in a single lattice of different species to both sides of the interface.

As an example, we consider one-dimensional heat transfer across a junction in a system of length L, with the junction in the middle. For simplicity, we consider this problem with the 9-moment system, in dimensionless coordinates. To be specific, we split the system into the domain a, where $x \in \left(-\frac{1}{2}, 0\right)$, and the domain b, where $x \in \left(0, \frac{1}{2}\right)$. The integrated momentum balance in domains a and b reads

$$e = 3C_a - 3\frac{px}{\mathrm{Kn}_\mathrm{R}^a}, \qquad e = 3C_b - \frac{3px}{\mathrm{Kn}_R^b} \tag{70}$$

where p is the constant energy flux, $\frac{1}{3}\mathrm{Kn}_\mathrm{R}^{a,b}$ are the dimensionless heat conductivities in the domains, and $C_{a,b}$ are constants of integration. The boundary conditions for domain a are

$$p = -\frac{1}{2}\frac{1-\alpha_a}{1+\alpha_a}(e - E_-) \qquad \text{at } x = -\frac{1}{2},$$
$$p = \frac{1}{2}\frac{1-\alpha_{a,j}}{1+\alpha_{a,j}}(e - E_0) \qquad \text{at } x = 0,$$

where α_a and $\alpha_{a,j}$ are the scattering coefficients at the left boundary and the junction, respectively, E_- is the energy prescribed at the left boundary, and E_0 is the unknown energy of the junction. In domain b, the boundary conditions are correspondingly

$$p = -\frac{1}{2}\frac{1-\alpha_{b,j}}{1+\alpha_{b,j}}(e - E_0) \qquad \text{at } x = 0,$$
$$p = \frac{1}{2}\frac{1-\alpha_b}{1+\alpha_b}(e - E_+) \qquad \text{at } x = \frac{1}{2}.$$

The constants of integration of the problem are the energy flux p, the junction energy E_0, and the constants C_a, C_b. The solution is straightforward; for the energy flux and the energy of the junction, we find

$$\begin{aligned} p &= \frac{\frac{1}{2}(E_- - E_+)}{\frac{3}{4}\frac{1}{\mathrm{Kn}_\mathrm{R}^a} + \frac{1+\alpha_a}{1-\alpha_a} + \frac{1+\alpha_{a,j}}{1-\alpha_{a,j}} + \frac{3}{4}\frac{1}{\mathrm{Kn}_\mathrm{R}^b} + \frac{1+\alpha_b}{1-\alpha_b} + \frac{1+\alpha_{b,j}}{1-\alpha_{b,j}}}, \\ E_0 &= \frac{E_+\left(\frac{3}{4}\frac{1}{\mathrm{Kn}_\mathrm{R}^a} + \frac{1+\alpha_a}{1-\alpha_a} + \frac{1+\alpha_{a,j}}{1-\alpha_{a,j}}\right) + E_-\left(\frac{3}{4}\frac{1}{\mathrm{Kn}_\mathrm{R}^b} + \frac{1+\alpha_b}{1-\alpha_b} + \frac{1+\alpha_{b,j}}{1-\alpha_{b,j}}\right)}{\frac{3}{4}\frac{1}{\mathrm{Kn}_\mathrm{R}^a} + \frac{1+\alpha_a}{1-\alpha_a} + \frac{1+\alpha_{a,j}}{1-\alpha_{a,j}} + \frac{3}{4}\frac{1}{\mathrm{Kn}_\mathrm{R}^b} + \frac{1+\alpha_b}{1-\alpha_b} + \frac{1+\alpha_{b,j}}{1-\alpha_{b,j}}} \end{aligned} \tag{71}$$

and the energy in domains a and b is

$$\begin{aligned} e(x) &= E_- - \frac{\left(\frac{3}{2\mathrm{Kn}_\mathrm{R}^a}\left(\frac{1}{2}+x\right) + \frac{1+\alpha_a}{1-\alpha_a}\right)(E_- - E_+)}{\frac{3}{4}\frac{1}{\mathrm{Kn}_\mathrm{R}^a} + \frac{1+\alpha_a}{1-\alpha_a} + \frac{1+\alpha_{a,j}}{1-\alpha_{a,j}} + \frac{3}{4}\frac{1}{\mathrm{Kn}_\mathrm{R}^b} + \frac{1+\alpha_b}{1-\alpha_b} + \frac{1+\alpha_{b,j}}{1-\alpha_{b,j}}}, \quad x \le 0 \\ e(x) &= E_+ + \frac{\left(\frac{3}{2\mathrm{Kn}_\mathrm{R}^b}\left(\frac{1}{2}-x\right) + \frac{1+\alpha_b}{1-\alpha_b}\right)(E_- - E_+)}{\frac{3}{4}\frac{1}{\mathrm{Kn}_\mathrm{R}^a} + \frac{1+\alpha_a}{1-\alpha_a} + \frac{1+\alpha_{a,j}}{1-\alpha_{a,j}} + \frac{3}{4}\frac{1}{\mathrm{Kn}_\mathrm{R}^b} + \frac{1+\alpha_b}{1-\alpha_b} + \frac{1+\alpha_{b,j}}{1-\alpha_{b,j}}}, \quad x \ge 0 \end{aligned} \tag{72}$$

As an example for the influence of the junction on heat transfer, we consider a system where $\alpha_a = \alpha_b = 0.5$ at the outer boundaries and $\alpha_{a,j} = \alpha_{b,j} = \alpha_j$ at the junction; the Knudsen numbers in both domains are the same, $\mathrm{Kn}_\mathrm{R}^a = \mathrm{Kn}_\mathrm{R}^b = \mathrm{Kn}_\mathrm{R}$. Figure 6 shows the influence of the interface parameter α_j on the dimensional heat flux p (with $E_- = 1.05$, $E_+ = 0.95$). The junction lowers heat transfer considerably for larger Knudsen numbers, the more so when the reflection rate α_j is larger.

For some insight into the energy distribution, we consider the case where $\mathrm{Kn}_\mathrm{R}^a = \mathrm{Kn}_\mathrm{R}^b = 0.1$, and the other parameters are as before, shown in Fig. 7. We observe energy jumps at the junction and the outer boundaries. The jump at the junction increases with the reflection coefficient α_j.

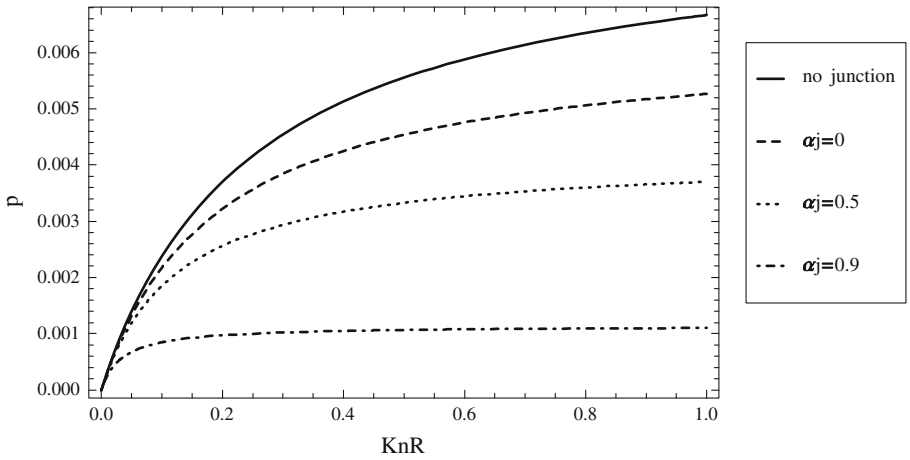

Fig. 6 Total dimensionless heat flux p in a system with junction for various interface parameters α_j as function of the Knudsen number $\mathrm{Kn_R} = \mathrm{Kn_R^a} = \mathrm{Kn_R^b}$. Other parameters are $\alpha_a = \alpha_b = 0.5,\ E_- = 1.05,\ E_+ = 0.95$

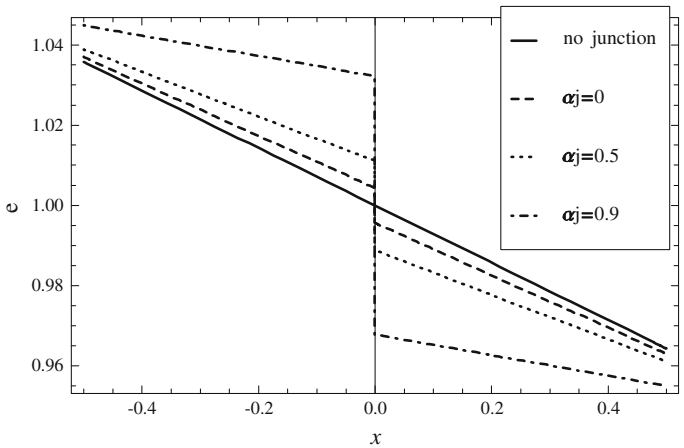

Fig. 7 Dimensionless energy $e\,(x)$ in a system with junction for various interface parameters α_j. Other parameters are $\mathrm{Kn_R^a} = \mathrm{Kn_R^b} = 0.1, \alpha_a = \alpha_b = 0.5,\ E_- = 1.05,\ E_+ = 0.95$

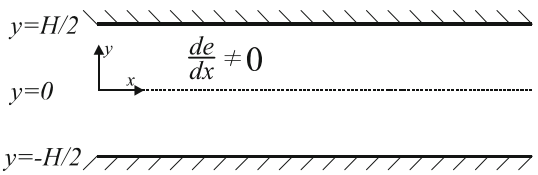

Fig. 8 One-dimensional Poiseuille flow

5.3 1-D Poiseuille flow

Another problem for which an analytical solution can be obtained is one-dimensional Poiseuille flow in a heat conductor of thickness H. In this case, there is a constant energy gradient $\frac{\partial e}{\partial x}$ in the x-direction inside a semi-infinite solid with adiabatic boundaries at $y = \pm\frac{H}{2}$ (see Fig. 8 for the geometry). This flow is analogous to pressure-driven flow in fluid dynamics (see, e.g., Ref. [26] for a discussion of Poiseuille flow in rarefied gases).

The simplified equations for the 25-moment case to describe this problem read

$$\begin{aligned}
\frac{1}{3}\frac{\partial e}{\partial x}+\frac{\partial N_{\langle xy\rangle}}{\partial y} &= -\frac{1}{\mathrm{Kn_R}}p_x \\
\frac{1}{5}\frac{\partial p_x}{\partial y}+\frac{\partial M_{\langle xyy\rangle}}{\partial y} &= -\frac{1}{\mathrm{Kn}}N_{\langle xy\rangle} \\
\frac{8}{35}\frac{\partial N_{\langle xy\rangle}}{\partial y}+\frac{\partial R_{\langle xyyy\rangle}}{\partial y} &= -\frac{1}{\mathrm{Kn}}M_{\langle xyy\rangle} \\
\frac{5}{21}\frac{\partial M_{\langle xyy\rangle}}{\partial y} &= -\frac{1}{\mathrm{Kn}}R_{\langle xyyy\rangle}
\end{aligned} \tag{73}$$

We have introduced dimensionless variables, such that $c=1,\ H=1$; the Knudsen numbers are formed with the channel height, $\mathrm{Kn_R}=\frac{\tau_\mathrm{R}}{H/c}$, $\mathrm{Kn}=\frac{\tau}{H/c}$. The relevant boundary conditions are

$$\begin{aligned}
N_{\langle xy\rangle} &= -\nu\frac{3}{8}\frac{1-\gamma}{1+\gamma}\left[p_x+\frac{35}{12}M_{\langle xyy\rangle}\right]+\frac{3}{2}R_{\langle xyyy\rangle}, \\
R_{\langle xyyy\rangle} &= \nu\frac{3}{4}\frac{1-\gamma}{1+\gamma}\left[p_x+\frac{105}{16}M_{\langle xyy\rangle}\right]+\frac{18}{7}N_{\langle xy\rangle}.
\end{aligned} \tag{74}$$

where ν is 1 at the lower boundary and -1 at the upper boundary. Note that adiabatic boundaries require that no thermalization occurs, that is, $\alpha=1$.

The solution for this problem is straightforward for all moment numbers considered. For the 4-moment case, the boundaries have no influence, and the heat flux is constant across the system,

$$p_4=-\frac{\mathrm{Kn_R}}{3}\frac{\partial e}{\partial x}. \tag{75}$$

In the 9-moment case, due to isotropic scattering at the boundary, the phonon flow experiences drag at the boundary, which leads to a Knudsen layer correction. With the abbreviation $\lambda_9=\sqrt{\frac{1}{5}\mathrm{Kn_R Kn}}$, the solution reads

$$p_9=-\frac{\mathrm{Kn_R}}{3}\frac{\partial e}{\partial x}\left(1-\frac{1}{1+\frac{8}{3}\frac{1+\gamma}{1-\gamma}\frac{\lambda_9}{\mathrm{Kn_R}}\tanh\left[\frac{1}{2\lambda_9}\right]}\frac{\cosh\left[\frac{y}{\lambda_9}\right]}{\cosh\left[\frac{1}{2\lambda_9}\right]}\right), \tag{76}$$

Note that for a specularly reflecting wall, where $\gamma=1$, the Knudsen layer vanishes.

The solution for the 16-moment case is rather similar, with a single Knudsen layer. With the abbreviation $\lambda_{16}=\sqrt{\mathrm{KnKn}_R\frac{1}{5}\left(1+\frac{8}{7}\frac{\mathrm{Kn}}{\mathrm{Kn_R}}\right)}$, the solution reads

$$p_{16}=-\frac{\mathrm{Kn_R}}{3}\frac{\partial e}{\partial x}\left(1-\frac{1}{1+\frac{2}{3}\frac{\mathrm{Kn}}{\mathrm{Kn_R}}+\frac{8}{3}\frac{1+\gamma}{1-\gamma}\frac{\lambda_{16}}{\mathrm{Kn_R}}\tanh\left[\frac{1}{2\lambda_{16}}\right]}\frac{\cosh\left[\frac{y}{\lambda_{16}}\right]}{\cosh\left[\frac{1}{2\lambda_{16}}\right]}\right) \tag{77}$$

Comparison with the 9-field case shows that the difference between the two solutions vanishes when there are far more normal processes as compared to resistive processes, so that $\frac{\mathrm{Kn}}{\mathrm{Kn_R}}\ll 1$.

Finally, the 25-moment equation adds a second Knudsen layer. With the abbreviation

$$\lambda_{25a,b}=\sqrt{\frac{1}{2}\mathrm{KnKn}_R\left(\left(\frac{1}{5}+\frac{7}{15}\frac{\mathrm{Kn}}{\mathrm{Kn_R}}\right)\pm\frac{1}{5}\sqrt{1-\frac{2}{21}\frac{\mathrm{Kn}}{\mathrm{Kn_R}}+\frac{49}{9}\frac{\mathrm{Kn}^2}{\mathrm{Kn_R}^2}}\right)} \tag{78}$$

the solution can be written as

$$p_{25}=-\frac{1}{3}\mathrm{Kn_R}\frac{\partial e}{\partial x}\left(1-C_1\cosh\frac{y}{\lambda_{25a}}-C_2\cosh\frac{y}{\lambda_{25b}}\right) \tag{79}$$

where the expressions for the constants of integration C_1 and C_2 are too lengthy to show here.

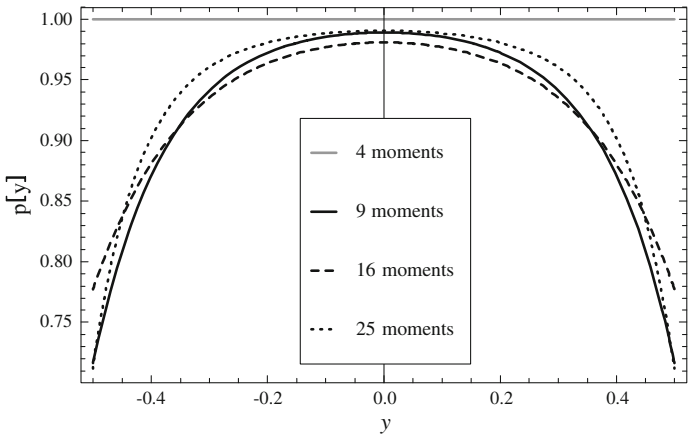

Fig. 9 Poiseuille flow solutions for the 4-, 9-, 16-, and 25-moment equations with Kn $= 0.2$, $\mathrm{Kn_R} = 2\mathrm{Kn}$, $\alpha = 1$, and $\gamma = 0.5$

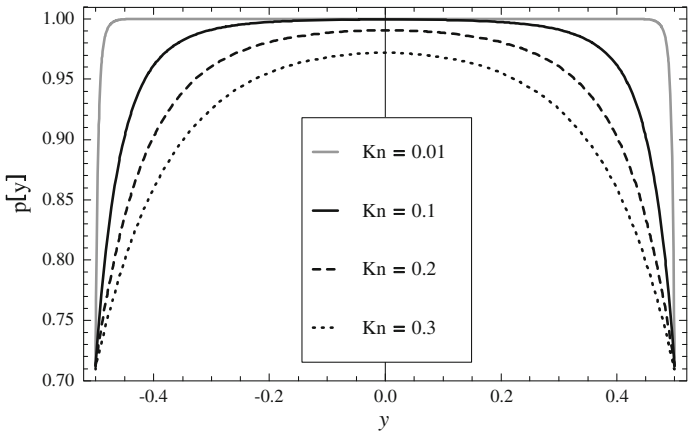

Fig. 10 The 25-moment solution to phonon Poiseuille flow for various Knudsen numbers. In all cases $\mathrm{Kn_R} = 2\mathrm{Kn}$, $\alpha = 1$, and $\gamma = 0.5$. At low Knudsen number, the solution approaches Fourier's law (plug flow). At higher Knudsen numbers, drag induced at the boundary becomes apparent

Figure 9 shows the phonon heat flux (= momentum, since $c = 1$) for Fourier's law (4 moments) and the 9-, 16-, and 25-moment equations for $Kn = 0.2$, normalized with the Fourier heat flux $p_4 = -\frac{\mathrm{Kn_R}}{3}\frac{\partial e}{\partial x}$. The graph shows well-developed Knudsen layers for the larger moment sets, which differ in detail but are relatively similar.

Figure 10 shows the effect that the Knudsen number has on the solution, for the 25-moment case. As Knudsen number decreases, the 25-moment solution approaches plug flow, as would be expected from Fourier's law, which indeed is valid for this case. At higher Knudsen numbers, the Knudsen layer becomes more apparent as boundary effects begin to dominate the solution.

The Knudsen layer is also affected by the relative proportion γ of scattered and specularly reflected phonons as shown in Fig. 11. As the proportion of scattered phonons is increased, the drag on the boundary becomes more dominant, increasing the size of the Knudsen layer. If more phonons are specularly reflected, the Knudsen layer diminishes. It is important to note that even though pure specular reflection achieves plug flow and the same result as Fourier's law, this effect is independent of Fourier heat conduction. The Fourier solution has plug flow no matter what proportion of phonons are scattered or reflected.

Much like the heated parallel plates' problem, a relative heat conductivity can be defined for the Poiseuille flow case by integrating the phonon heat flux over the domain to get the total heat flux

$$P = \int_{-1/2}^{1/2} p\,(y)\,\mathrm{d}y. \tag{80}$$

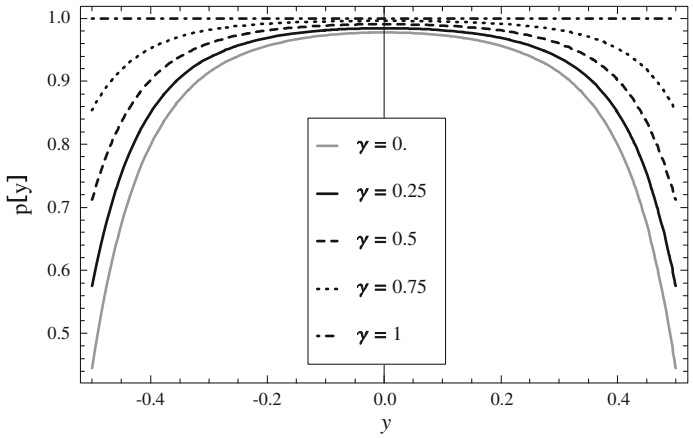

Fig. 11 The 25-moment solution to Poiseuille flow for various values of γ. In all cases Kn $= 0.2$, $\text{Kn}_\text{R} = 2\text{Kn}$, and $\alpha = 1$. Phonon drag at the boundary is influenced by the proportion of phonons that scatter and reflect. In the case of specular reflection ($\gamma = 1$), plug flow is achieved, while drag is increased as scattering increases

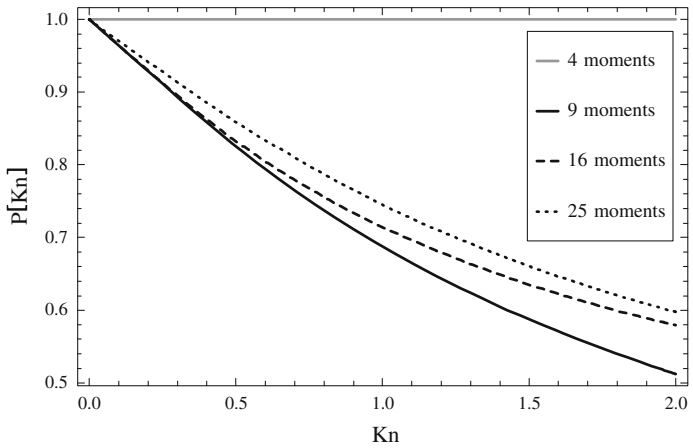

Fig. 12 Relative heat conductivity for the 9-, 16-, and 25-moment equations compared to Fourier's law for Poiseuille flow. In all cases, $\text{Kn}_\text{R} = 2\text{Kn}$, $\alpha = 1$, and $\gamma = 0.5$

In Fig. 12, we see that as Knudsen number increases, the relative heat conductivity, defined as the ratio of the total energy flux to the 4-moment case (Fourier's law), P/P_4, decreases because of phonon drag in the Knudsen layer. The reduction in conductivity is significant, in particular for narrow devices, where the Knudsen number is larger. We note that the results are for $\gamma = 0.5$, so that a significant portion of boundary interactions are specular reflections. If isotropic scattering is more dominant, so that γ is smaller, conductivity is even smaller. Figure 12 shows that the different moment sets give the same energy flow only at small Knudsen numbers, but give different values as Kn becomes larger. Since higher moment numbers typically give a finer resolution, we expect that the result for 25 moments is more realistic.

6 Conclusion and recommendations

At very small phonon Knudsen number, heat transfer is governed by Fourier's law. As Knudsen number increases, nonequilibrium effects become more significant, making Fourier's law increasingly inaccurate. For a more accurate set of transport equations, a microscopic analysis of heat transfer is needed.

Phonons are quasiparticles derived from quantum mechanics representing lattice vibrations of particles relative to their mean position. All phonon interactions conserve energy, but they do not always conserve quasimomentum. Phonon gas kinetics can be described using the phonon Boltzmann equation; however, its nonlinear characteristics make it difficult to solve on its own. The Boltzmann equation can be approximated by taking a finite number of moments of the equation to develop macroscopic transport equations.

We presented a set of linear transport equations based on several assumptions: The phonon dispersion relation was assumed to be linear with an infinite Brillouin zone. The gray matter Callaway model was used to approximate the phonon collision term on the right-hand side of the Boltzmann equation. The Grad moment closure was used to reduce the number of unknown variables to make the system of equations well posed.

Boundary conditions were derived by considering three simple microscopic interactions with the crystal boundary: thermalization, isotropic scattering, and specular reflection. The boundary conditions are set up so that the proportion of phonons in each interaction can be easily changed to match known conditions or other models. The microscopic boundary conditions were integrated to create boundary conditions for the macroscopic transport equations. The boundary conditions were reduced using Grad's boundary reduction method so that there would not be too many boundary conditions for the number of constants of integration. Boundary conditions were macroscopically derived for an arbitrary number of moments in three dimensions.

Analytic solutions for simple geometries can be determined with the transport equations. One-dimensional heat transfer and Poiseuille flow were both solved in one dimension for the 4-, 9-, 16-, and 25-moment equations and compared with each other. The solutions depend on the Knudsen number; cases with small Knudsen number had solutions similar to Fourier's law, while rarefaction effects became apparent as Knudsen number got larger. As Kn is increased, the temperature jump (and slip) at the wall increases and the Knudsen layer becomes larger. The cumulative effect of rarefaction is an overall decrease in heat flux, which can be related to Fourier heat flux by defining a relative heat conductivity for systems with large Knudsen number.

The macroscopic transport equations for phonons in a solid are a simple and efficient way for solving nonequilibrium heat transfer systems, but more research is necessary to both improve the model and compare it to existing models and experiments. In particular, the model must be improved by removing some of the assumptions used: Use of a realistic nonlinear dispersion relation for phonons, and consideration of the finite Brillouin zone will better approximate reality and will also increase the model's usefulness to regimes above the Debye temperature. Removing the gray matter assumption for the Callaway model will lead to a more realistic description of moment relaxation. Experimental data have shown that mean free path can be strongly dependent on wave vector and that this is important for overall heat transfer properties in nonequilibrium systems [27]. Considering the proper frequency-dependent relaxation times in the Callaway model will add another nonlinearity to the system. We have developed and used appropriate methods in classical kinetic theory [28,29], where the resulting macroscopic equations give meaningful results as long as the Knudsen number does not get too large [26,30]. The same ideas will be used in the future for kinetic theory of phonons to derive a reliable set of macroscopic moment equations which then should paint a more realistic picture.

Verification of the moment method is necessary. A first step would be to compare the model with solutions of the phonon Boltzmann equation, e.g., by means of the DSMC [4]. Comparison with experimental results can be used to determine transport parameters for the equations, such as temperature dependence of relaxation times, and the parameters in the boundary conditions. These comparisons should be done for refined moment equations that are derived accounting for the detailed frequency-dependent behavior; hence, they are left for future work.

Acknowledgments This research was supported by the Natural Sciences and Engineering Research Council (NSERC).

Appendix A: Computation of the scattering integral from Grad distribution

In this Appendix, we determine the integral in (29) with the Grad distribution (27), that is,

$$f_{\mathrm{G,scatter}} = \frac{1}{\pi c} \int\limits_{n_k \nu_k < 0} c\,(-n_k \nu_k)\, f_{\mathrm{G}} \mathrm{d}\Omega$$

Insertion of the expression of f_{G} and simplification gives at first

$$f_{\mathrm{G,scatter}} = f_{\mathrm{Bose}} - \frac{\partial f_{\mathrm{Bose}}}{\partial k} \frac{ck}{aT^4} \sum_{n=1}^{N} \frac{(2n+1)!!}{4n!} u_{\langle i_1 \cdots i_n \rangle} \frac{1}{\pi} \int\limits_{n_k \nu_k < 0} (-n_k \nu_k)\, n_{i_1} \cdots n_{i_n} \mathrm{d}\Omega,$$

we used the identity $u_{\langle i_1 \cdots i_n \rangle} n_{\langle i_1} \cdots n_{i_n \rangle} = u_{\langle i_1 \cdots i_n \rangle} n_{i_1} \cdots n_{i_n}$.
For further evaluation, we now chose coordinates where the surface normal points into the 3-direction, so that $\nu_i = \{0, 0, 1\}_i$. For the phonon direction vector, we write $n_k = \{\tau_A, \nu\}_k$ with the normal component

$\nu = n_k \nu_k = \cos\theta$ and the tangential vector $\tau_A = \{\sin\theta\cos\phi, \sin\theta\sin\phi\}$; hence, we use capital indices for the 2-D tangential components. With this notation, we can write tensors in terms of normal and tangential components. For instance, the second-order moment $u_{\langle ij\rangle}$ can be written as

$$u_{\langle ij\rangle} = \begin{bmatrix} u_{\langle AB\rangle} & u_{\langle A\nu\rangle} \\ u_{\langle \nu B\rangle} & u_{\langle \nu\nu\rangle} \end{bmatrix}_{ij}$$

with the trace-free condition $u_{\langle AA\rangle} + u_{\langle \nu\nu\rangle} = 0$, and, because of symmetry, $u_{\langle A\nu\rangle} = u_{\langle \nu A\rangle}$. Extension to higher-order tensors is evident. With this notation, we have

$$u_{\langle i_1\cdots i_n\rangle} n_{i_1}\cdots n_{i_n} = \sum_{r=0}^{n} \frac{n!}{r!\,(n-r)!} u_{\langle A_1\cdots A_r \nu\cdots\nu\rangle} \tau_{A_1}\cdots\tau_{A_r}\nu^{n-r},$$

and accordingly

$$f_{\mathrm{G,scatter}} = f_{\mathrm{Bose}} + \frac{\partial f_{\mathrm{Bose}}}{\partial k}\frac{ck}{aT^4}\sum_{n=1}^{N}\frac{(2n+1)!!}{4n!}\sum_{r=0}^{n}\frac{n!}{r!\,(n-r)!}u_{\langle A_1\cdots A_r\nu\cdots\nu\rangle}\frac{1}{\pi}\int\limits_{\nu<0}\tau_{A_1}\cdots\tau_{A_r}\nu^{n-r+1}\mathrm{d}\Omega.$$

The integral has contributions only for even number of tangential indices r, and it must be an isotropic tensor. We write

$$\frac{1}{\pi}\int\limits_{\nu<0}\tau_{A_1}\cdots\tau_{A_r}\nu^{n-r+1}\mathrm{d}\Omega = \begin{cases} \sigma_r^n \delta_{\{A_1A_2\cdots A_r\}} & (r \text{ even}) \\ 0 & (r \text{ odd}) \end{cases} \tag{81}$$

Here, $\delta_{\{A_1A_2\cdots A_r\}}$ is a generalized tangential unit tensor which has $(r-1)!!$ terms, e.g.,

$$\begin{aligned} \delta_{\{AB\}} &= \delta_{AB} \\ \delta_{\{ABCD\}} &= \delta_{AB}\delta_{CD} + \delta_{AC}\delta_{BD} + \delta_{AD}\delta_{BC} \end{aligned} \tag{82}$$

For the traces of these, we find the rules

$$\begin{aligned} \delta_{AA} &= 2 \\ \delta_{\{A_1A_2\cdots A_r\}}\delta_{A_{r-1}A_r} &= r\delta_{\{A_1A_2\cdots A_{r-2}\}} \\ \delta_{\{A_1A_2\cdots A_r\}}\delta_{A_1A_2}\cdots\delta_{A_{r-1}A_r} &= \prod_{k=0}^{\frac{r-2}{2}}(r-2k) = r!! \end{aligned}$$

By taking $\frac{r}{2}$ traces in (81), we find for the coefficients (r even), with $\tau_A\tau_A = \tau^2 = \sin^2\theta$, $\nu = \cos\theta$ and $\mathrm{d}\Omega = \sin\theta d\theta\mathrm{d}\phi$,

$$\sigma_r^n = \frac{1}{\pi r!!}\int_{\theta=\frac{\pi}{2}}^{\pi}\int_{\phi=0}^{2\pi}\sin^{r+1}\theta\cos^{n-r+1}\theta\mathrm{d}\theta\mathrm{d}\phi = (-1)^{n-r+1}\frac{\Gamma\left(1+\frac{n-r}{2}\right)\Gamma\left(1+\frac{r}{2}\right)}{r!!\Gamma\left(2+\frac{n}{2}\right)}$$

We also need to consider the tensor product

$$u_{\langle A_1\cdots A_r\nu\cdots\nu\rangle}\delta_{\{A_1A_2\cdots A_r\}} = (r-1)!!u_{\langle A_1A_1\cdots A_{r/2}A_{r/2}\nu\cdots\nu\rangle} = (r-1)!!\,(-1)^{\frac{r}{2}}\,u_{\langle\nu\cdots\nu\rangle|n}$$

where the subscript n denotes the moment with n indices. Then

$$f_{\mathrm{G,scatter}} = f_{\mathrm{Bose}} - \frac{\partial f_{\mathrm{Bose}}}{\partial k}\frac{ck}{4aT^4}\sum_{n=1}^{N}\vartheta_n u_{\langle\nu\cdots\nu\rangle|n}. \tag{83}$$

with the full normal components of the moments

$$u_{\langle\nu\cdots\nu\rangle|n} = u_{\langle i_1\cdots i_n\rangle}\nu_{i_1}\cdots\nu_{i_n}$$

and the coefficient

$$\vartheta_n = \sum_{\substack{r=0 \\ r \text{ even}}}^{n} (-1)^{n-\frac{r}{2}} \frac{(r-1)!!}{r!!} \frac{(2n+1)!!\left(\frac{r}{2}\right)!}{r!\,(n-r)!} \frac{\Gamma\left(1+\frac{n-r}{2}\right)}{\Gamma\left(2+\frac{n}{2}\right)}, \tag{84}$$

which has the values

$$\vartheta_n = \left\{1, -2, \frac{15}{8}, 0, -\frac{105}{64}, 0, \frac{3003}{1024}, 0, -\frac{109395}{16384}, 0, \cdots\right\} \tag{85}$$

Appendix B: Evaluation of Eq. (34)

We insert f_{B} and f_{G} into (35),

$$\int\limits_{n_k \nu_k > 0} k \tau_{A_1} \cdots \tau_{A_r} \nu^{n-r+1} \bar{f}\, \mathrm{d}\mathbf{k} = \int\limits_{n_k \nu_k > 0} k \tau_{A_1} \cdots \tau_{A_r} \nu^{n-r+1} f_{\mathrm{G}}\, \mathrm{d}\mathbf{k}; \tag{86}$$

With $\hat{n}_i = \left(n_i - 2 n_j \nu_j \nu_i\right)$ and $\mathrm{d}\mathbf{k} = k^2 \mathrm{d}k \mathrm{d}\Omega$, we obtain, after some reordering (cancel c), and use of the result of "Appendix A,"

$$\begin{aligned}
&(1-\alpha) \int \left(f_{\mathrm{Bose}}\left(T_{\mathrm{s}}, k\right) - f_{\mathrm{Bose}}\right) k^3 \mathrm{d}k \int\limits_{n_k \nu_k > 0} \tau_{A_1} \cdots \tau_{A_r} \nu^{n-r+1} \mathrm{d}\Omega \\
&-\alpha\gamma \sum_{m=1}^{N} \frac{(2m+1)!!}{4m!} \frac{c u_{\langle j_1 \cdots j_m \rangle}}{a T^4} \int \frac{\partial f_{\mathrm{Bose}}}{\partial k} k^4 \mathrm{d}k \int\limits_{n_k \nu_k > 0} \hat{n}_{\langle j_1} \cdots \hat{n}_{j_m \rangle} \tau_{A_1} \cdots \tau_{A_r} \nu^{n-r+1} \mathrm{d}\Omega \\
&-\alpha\left(1-\gamma\right) \frac{c}{4 a T^4} \sum_{m=1}^{N} \vartheta_m u_{\langle \nu \cdots \nu \rangle | m} \int \frac{\partial f_{\mathrm{Bose}}}{\partial k} k^4 \mathrm{d}k \int\limits_{n_k \nu_k > 0} \tau_{A_1} \cdots \tau_{A_r} \nu^{n-r+1} \mathrm{d}\Omega \\
&+\sum_{m=1}^{N} \frac{(2m+1)!!}{4m!} \frac{c u_{\langle j_1 \cdots j_m \rangle}}{a T^4} \int \frac{\partial f_{\mathrm{Bose}}}{\partial k} k^4 \mathrm{d}k \int\limits_{n_k \nu_k > 0} n_{\langle j_1} \cdots n_{j_m \rangle} \tau_{A_1} \cdots \tau_{A_r} \nu^{n-r+1} \mathrm{d}\Omega = 0.
\end{aligned}$$

The integrals over the Bose distribution give

$$\begin{aligned}
\int f_{\mathrm{Bose}} k^3 \mathrm{d}k &= \int \frac{y}{\exp \frac{\hbar c k}{k_B T} - 1} k^3 \mathrm{d}k = \frac{a T^4}{4\pi\hbar c} \\
\int \frac{\partial f_{\mathrm{Bose}}}{\partial k} k^4 \mathrm{d}k &= \left(\frac{k_B T}{\hbar c}\right)^4 \int \frac{\partial}{\partial x} \left(\frac{y}{\exp x - 1}\right) x^4 \mathrm{d}x = -\frac{a T^4}{\pi \hbar c}
\end{aligned}$$

Moreover, we introduce the decomposition into tangential and normal components of tensors,

$$\begin{aligned}
n_k \nu_k &= \nu \\
u_{\langle j_1 \cdots j_m \rangle} n_{j_1} \cdots n_{j_m} &= \sum_{s=0}^{m} \frac{m!}{s!\,(m-s)!} u_{\langle B_1 \cdots B_s \nu \cdots \nu \rangle | m} \tau_{B_1} \cdots \tau_{B_s} \nu^{m-s}
\end{aligned}$$

so that

$$\begin{aligned}
&\left[(1-\alpha)\left(a T_{\mathrm{s}}^4 - a T^4\right) + \alpha\left(1-\gamma\right) \sum_{m=1}^{N} \vartheta_m c u_{\langle \nu \cdots \nu \rangle | m}\right] \frac{1}{\pi} \int\limits_{\nu > 0} \tau_{A_1} \cdots \tau_{A_r} \nu^{n-r+1} \mathrm{d}\Omega \\
&-\sum_{m=1}^{N} \sum_{s=0}^{m} \left[1 - (-1)^{m-s} \alpha\gamma\right] \frac{(2m+1)!!}{s!\,(m-s)!} c u_{\langle B_1 \cdots B_s \nu \cdots \nu \rangle | m} \frac{1}{\pi} \int\limits_{\nu > 0} \tau_{A_1} \cdots \tau_{A_r} \tau_{B_1} \cdots \tau_{B_s} \nu^{n+m-r-s+1}\, \mathrm{d}\Omega = 0
\end{aligned}$$

The integrals are as in "Appendix A," only that integration is for different sign. We have

$$\frac{1}{\pi}\int\limits_{\nu>0} \tau_{A_1}\cdots\tau_{A_r}\nu^{n-r+1}\mathrm{d}\Omega = \begin{cases} \hat{\sigma}_r^n \delta_{\{A_1A_2\cdots A_r\}} & (r \text{ even}) \\ 0 & (r \text{ odd}) \end{cases}$$

with

$$\hat{\sigma}_r^n = \frac{1}{\pi r!!}\int\limits_{\theta=\frac{\pi}{2}}^{\pi}\int\limits_{\phi=0}^{2\pi} \sin^{r+1}\theta\cos^{n-r+1}\theta\mathrm{d}\theta\mathrm{d}\phi = \frac{\Gamma\left(1+\frac{n-r}{2}\right)\Gamma\left(1+\frac{r}{2}\right)}{r!!\Gamma\left(2+\frac{n}{2}\right)}. \tag{87}$$

Putting it all together, we finally obtain the result (38) given in the main text.

References

1. Romano, V., Rusakov, A.: 2d numerical simulations of an electron-phonon hydrodynamical model based on the maximum entropy principle. Comput. Methods Appl. Mech. Eng. **199**, 2741–2751 (2010)
2. Kittel, C.: Introduction to Solid State Physics, 7th edn. John Wiley & Sons, Hoboken (1996)
3. Snoke, D.W.: Solid State Physics Essential Concepts. Addison-Wesley, San Francisco (2009)
4. Peraud, J-P.M., Hadjiconstantinou, N.G.: Efficient simulation of multidimensional phonon transport using energy-based variance-reduced Monte Carlo formulations. Phys. Rev. B **84**, 205331 (2011)
5. Grad, H.: On the kinetic theory of rarefied gases. Commun. Pure Appl. Math. **2**, 331–407 (1949)
6. Dreyer, W., Struchtrup, H.: Heat pulse experiments revisited. Contin. Mech. Thermodyn. **5**, 3–50 (1993)
7. Alvarez, F.X., Jou, D., Sellitto, A.: Phonon hydrodynamics and phonon-boundary scattering in nanosystems. J. Appl. Phys. **105**, 014317 (2009)
8. Sellitto, A., Alvarez, F.X., Jou, D.: Second law of thermodynamics and phonon-boundary conditions in nanowires. J. Appl. Phys. **107**, 064302 (2010). doi:10.1063/1.3309477
9. Alvarez, F.X., Cimmelli, V.A., Jou, D., Sellitto, A.: Mesoscopic description of boundary effects in nanoscale heat transport. Nanoscale Syst. MMTA **1**, 112–142 (2012)
10. Guyer, R.A., Krumhansl, J.A.: Solution of the linearized phonon Boltzmann equation. Phys. Rev. **148**, 766–778 (1966)
11. Guyer, R.A., Krumhansl, J.A.: Thermal conductivity, second sound, and phonon hydrodynamic phenomena in nonmetallic crystals. Phys. Rev. **148**, 778–788 (1966)
12. Callaway, J.: Model for lattice thermal conductivity at low temperatures. Phys. Rev. **113**, 1046–1051 (1959)
13. Peierls, R.: Zur kinetischen Theorie der Wärmeleitung in Kristallen. Annalen der Physik **3**, 1055–1101 (1929)
14. Debye, P.: Zur Theorie der spezifischen Wärmen. Annalen der Physik **39**, 789–839 (1912)
15. Einstein, A.: Die Plancksche Theorie der Strahlung und die Theorie der spezifischen Wärme. Annalen der Physik **22**, 180–190 (1907)
16. Klemens, P.G.: Anharmonic decay of optical phonons. Phys. Rev. **148**, 845–848 (1966)
17. Waldmann, L.: Transporterscheinungen in Gasen von mittlerem Druck. In: Flügge, S. (ed.) Handbuch der Physik XII: Thermodynamik der Gase, Springer, Berlin (1958)
18. Struchtrup, H.: Macroscopic Transport Equations for Rarefied Gas Flows. Springer, Heidelberg (2005)
19. Müller, I.: Thermodynamics. Pitman Publishing, Boston (1985)
20. Bhatnagar, P.L., Gross, E.P., Krook, M.: A model for collision processes in gases. I. Small amplitude processes in charged and neutral one-component systems. Phys. Rev. **94**, 511–525 (1954)
21. Fryer, M.: The Macroscopic Transport Equations of Phonons in Solids. MASc thesis, University of Victoria (2012)
22. Torrilhon, M., Struchtrup, H.: Boundary conditions for regularized 13-moment-equations for micro-channel-flows. J. Comput. Phys. **227**, 1982–2011 (2008)
23. Struchtrup, H., Torrilhon, M.: Higher-order effects in rarefied channel flows. Phys. Rev. E **78**, 046301 (2008)
24. Hadjiconstantinou, N.G.: Comment on Cercignani's second-order slip coefficient. Phys. Fluids **15**, 2352–2354 (2003)
25. Struchtrup, H.: Linear kinetic heat transfer: moment equations, boundary conditions, and Knudsen layers. Physica A **387**, 1750–1766 (2008)
26. Taheri, P., Torrilhon, M., Struchtrup, H.: Couette and Poiseuille flows in microchannels: analytical solutions for regularized 13-moment equations. Phys. Fluids **21**, 017102 (2009)
27. Johnson, J.A., Maznev, A.A., Cuffe, J., Eilason, J.K., Minnich, A.J., Kehoe, T., Sotomayor Torres, C.M., Chen, G., Nelson, K.A.: Direct measurement of room temperature non-diffusive thermal transport over micron distance in a silicon membrane. Phys. Rev. Lett. **110**, 025901 (2013)
28. Struchtrup, H., Taheri, P.: Macroscopic transport models for rarefied gas flows: a brief review. IMA J. Appl. Math. **76**, 672–697 (2011)
29. Struchtrup, H., Torrilhon, M.: Regularized 13 moment equations for hard sphere molecules: linear bulk equations. Phys. Fluids **25**, 052001 (2013)
30. Rana, A.S., Torrilhon, M., Struchtrup, H.: A robust numerical method for the R13 equations of rarefied gas dynamics: application to lid driven cavity. J. Comput. Phys. **236**, 169–186 (2013)